

NSP-64-25

RIFT RADIATION EFFECTS PROGRAM

IRRADIATIONS NO. 5 AND 8 ELECTRICAL CABLES

Prepared under Contracts NAS 8-5600 and NAS 8-9500

Handwritten signature
LTO
IL Destroy
Office

FACILITY FORM 502	N64-29558	
	(ACCESSION NUMBER)	(THRU)
	<i>OK</i>	1
	(PAGE)	(CODE)
	CR-57229	27
	(NASA CR OR TMX OR AD NUMBER)	(CATEGORY)

Lockheed

MISSILES & SPACE COMPANY

A GROUP DIVISION OF LOCKHEED AIRCRAFT CORPORATION

OTS PRICE

SUNNYVALE, CALIFORNIA

XEROX \$ _____


MICROFILM \$ _____

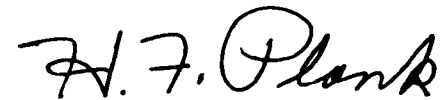
RIFT RADIATION EFFECTS PROGRAM

IRRADIATIONS NO. 5 AND 8 ELECTRICAL CABLES

Prepared under Contracts NAS 8-5600 and NAS 8-9500

Approved


A. J. STEELE, Mgr.
LSVP Engineering


H. F. PLANK, Director
Large Space Vehicle Programs
Space Programs Division

FOREWORD

This report describes work performed under Contract No. NAS 8-5600 for the George C. Marshall Space Flight Center as part of the Supporting R&D effort of the RIFT Program. Experimental work was performed for the Lockheed Missiles & Space Company by the Lockheed-Georgia Company at the Radiation Effects Facility, Dawsonville, Georgia. Acknowledgment is made specifically to LGC Reports ND 407, 24 May 1963, and ND 410, 5 July 1963.

ABSTRACT

~~2555~~

This report presents the test methods and analysis of results of cable irradiation tests 5 and 8 performed by Lockheed for the NASA RIFT program. The data herein were taken at a temperature of 70°C on radio-frequency noise for coaxial cables RG 58C/U and RG 141/U and the insulation conductance and photovoltaic current on cables RG 58C/U, RG 141/U, MD-324, COS-47831, PSC-C-39001-4-24 ST, RT 24(19)ST 2RO/9-0 and Bendix connector PT00P-14-5 S/PT06P-14-5 P.

~~auth~~

SUMMARY

29558

Presented herein are the results of measurements made during irradiation of: coaxial cables RG 58C/U and RG 141/U; multiconductor cables MD-324, CDS-47831, PSC-G-39001 and RT 24(19)ST; connector PT00P-14-5 S/PT06P-14-5 P.

These cables were tested at 70°C under radiation dose rates of 10^4 to 2×10^6 r/hr and at total doses to 3×10^7 r. Irradiations were performed at the Radiation Effects Reactor, Georgia Nuclear Laboratories.

The conductance and currents found for the minimum and maximum dose rates are shown in Table S-1. The empirical equations derived for slab geometry of dielectrics were not applicable to the majority of the data.

Author

Table S-1
CABLE IRRADIATION -- RESULTS AT 70°C

Cable Dose Rate (r/hr)	Conductance (ohm ⁻¹)		Current (amps)	
	10 ⁴	2x10 ⁶	10 ⁴	2x10 ⁶
RG 58C/U	6x10 ⁻¹³	2x10 ⁻¹¹	8x10 ⁻¹³	2x10 ⁻¹⁰
RG 141/U	2x10 ⁻¹³	4x10 ⁻¹⁰	4x10 ⁻¹²	2x10 ⁻⁹
MD 324	4x10 ⁻¹⁴	5x10 ⁻¹³	3x10 ⁻¹³	5x10 ⁻¹²
CDS 47831	6x10 ⁻¹¹	4x10 ⁻¹⁰	2.9x10 ⁻¹¹	5.0x10 ⁻¹¹
PSC-C-39001	6x10 ⁻¹³	8x10 ⁻¹¹	—	—
RT 24(19)ST	2x10 ⁻¹³	1x10 ⁻¹²	2x10 ⁻¹²	8x10 ⁻¹¹
PT00P-14-5 S/ PT06P-14-5 P	2x10 ⁻⁹	1x10 ⁻⁸	4x10 ⁻¹⁰	5x10 ⁻⁹

- No noise above 10 db was detected during the radio frequency noise test at 400 megacycles for the cables RG 58C/U and RG 141/U.
- Values of conductance and current measured indicate that cable radiation effects should not present an engineering problem at RIFT dose levels in stage applications where impedances are normally low and signal levels are in the normal millivolt range.

CONTENTS

<u>Section</u>		<u>Page</u>
	FOREWORD	iii
	ABSTRACT	v
	SUMMARY	vii
1	INTRODUCTION	1-1
2	TEST OBJECTIVES	2-1
3	TEST DESCRIPTION	3-1
	3.1 Test Specimens	3-1
	3.2 Test Equipment	3-12
	3.3 Test Procedures	3-17
4	RESULTS	4-1
	4.1 Environmental Data	4-1
	4.2 Data Reduction	4-14
	4.3 Experimental Results	4-19
	4.4 Further Discussion of Results	4-44
5	CONCLUSIONS	5-1
6	REFERENCES	6-1

ILLUSTRATIONS

Figure		Page
3-1	Instrumentation Cabling	3-2
3-2	Insulation Conductance and Photovoltaic Current Measurement	3-14
3-3	R-F Noise Measurement	3-15
3-4	Test Flow Diagram	3-18
3-5	Mounting for Cable Specimens	3-21
3-6	Mounting for Cable and Connector Specimens	3-22
4-1	Irradiation 5 -- Temperature History of Test Specimens	4-2
4-2	Irradiation 8 -- Temperature History of Test Specimens	4-3
4-3	Irradiation 5 -- Test Panel Plan with Gamma Dose-Rate Isodose	4-5
4-4	Irradiation 8 -- Test Panel with Gamma Dose-Rate Isodose	4-7
4-5	Irradiation 5 -- Fast Neutron Flux above Effective Threshold Energy	4-11
4-6	Irradiation 8 -- Fast Neutron Flux above Effective Threshold Energy	4-12
4-7	Gamma-Ray Energy Spectrum of the RER	4-13
4-8	Leakage Conductance per Lineal Foot vs Gamma Rate -- RG-58C/U	4-21
4-9	Leakage Conductance per Lineal Foot vs Gamma Rate -- RG-141	4-23
4-10	Photovoltaic Current per Lineal Foot vs Gamma Rate -- Coaxial Cable	4-25
4-11	Conductance of RG-58C/U Cable at 12 and 70°C	4-27
4-12	Leakage Conductance between Shield and Conductor per Lineal Foot of Cable Type MD 324 vs Gamma Rate	4-29

ILLUSTRATIONS (Continued)

<u>Figure</u>		<u>Page</u>
4-13	Leakage Conductance between Shield and Conductor per Lineal Foot of Cable Type CDS 47831 (PVC) vs Gamma Rate	4-31
4-14	Photovoltaic Current between Shield and Conductor per Lineal Foot of Cable Type CDS 47831	4-34
4-15	Leakage Conductance between Shield and Conductor per Lineal Foot of Cable Type PSC-C-39001-4-24ST	4-35
4-16	Leakage Conductance between Shield and Conductor per Lineal Foot of Cable Type RT 24(19)ST-2R0/9-0	4-37
4-17	Photovoltaic Current between Shield and Conductor per Lineal Foot of Cable Type RT(19) ST-2R0/9-0	4-38
4-18	Leakage Conductance between Shield and Conductors per Connector Types PT 00P-14-5S and PT 06P-14-5P	4-39
4-19	Photovoltaic Current between Shield and Conductors per Connector Type PT 06P-14-5P	4-41

TABLES

<u>Table</u>		<u>Page</u>
S-1	Cable Irradiation -- Results at 70°C	viii
3-1	Test 5 -- Specimen Manufacturer's Specifications (nominal)	3-3
3-2	Test 5 -- Specimen History	3-5
3-3	Test 5 -- Specimen Summary	3-7
3-4	Test 8 -- Specimen Manufacturer's Specifications (nominal)	3-9
3-5	Test 8 -- Specimen History	3-11
3-6	Test 8 -- Specimen Summary	3-13
4-1	Test 5 -- Radiation Environment, Nominal Radiation Levels	4-9
4-2	Test 8 -- Radiation Environment, Actual Radiation Levels	4-10
4-3	Effect of Temperature on Cable Current (amperes)	4-43

Section 1 INTRODUCTION

When electrical cables are exposed to reactor radiations, charge carriers are produced in the cable insulating material (between conductors) by high energy gamma and neutron radiation; as a result, leakage currents increase as radiation exposure-rate increases. These radiations also generate photovoltages across the conductor-insulator and insulator-shield interfaces. Such radiation rate effects are coupled with permanent changes whose net effect is one of accelerated aging of the insulating material. For moderate radiation doses, the transient effects are more important than permanent effects because the temporary changes in properties, such as insulation electrical conductivity, are usually much greater than the residual or permanent changes observed (Ref. 1).

The RIFT Program needed engineering data on the transient effects of nuclear radiation on electrical cables. Total dose effects, on the other hand, were of less concern because considerable information is available on the accumulated dose effects on electrical insulation and total dose on RIFT cables will be relatively small in comparison to permanent damage threshold doses (with the possible exception of Teflon). The work done and reported by others on transient effects of radiation on cables has indicated that a problem may exist in low-signal-level or high-impedance circuits due to photo induced noise currents. The work reported in this area comes generally from three main sources: H. W. Wicklein, Boeing (Ref. 2), J. A. J. van Lint, General Dynamics (Ref. 3), and S. E. Harrison, Sandia (Ref. 4). Most of the work done by these three groups has been at very high dose rates in pulsed reactors; however, some steady-state results have been presented. Wicklein's data are all from high-power pulses and by itself, could not be reliably extrapolated for use on RIFT. Van Lint's data is mostly at high-pulse powers,

but some data is given at steady state conditions. These data are limited in scope, applying only to polyethylene-insulated RG-58/U coaxial cable. Van Lint attempted to determine and describe the physical reaction causing the transient effects. This effort, while of great intrinsic value, did not provide RIFT with the engineering data needed to evaluate or select specific instrumentation cables for the RIFT vehicle. Harrison's data, while quite complete and covering many dielectric materials, embraces only that area of radiation-induced photoconductivity. Only dielectric material samples were treated, and cables were not included. The photoconductivity behavior has some concern for RIFT, but the concurrently produced photocurrent is of great interest in this application. In brief, then, the above data cover photoconductivity of a wide range of dielectric materials, very-high-rate photocurrent data on polyethylene cables, and moderate-rate photocurrent data on only polyethylene cables.

Since there is no proved and reliable method to extrapolate these data, a series of tests was conducted to determine the effects of radiation rate on cables and connectors for potential RIFT applications. The results of the first two irradiations are reported in Ref. 5.

In the first test, conducted at ambient temperatures, insulation resistance and the ac and dc components of noise were measured on multiple samples of each of three types of coaxial cables — RG-58C/U, Microdot 50-3804, and Twinax RG-22/U — during exposures to gamma dose rates ranging from 10^4 to 10^6 r/hr. The insulation resistance decreased and the dc noise across large termination resistances increased as the radiation exposure rate increased. No ac noise voltages were observed.

The second test was also conducted at ambient temperatures. Samples of four types of coaxial cables, RG-8A/U, RG-58C/U, RG-141/U and RG-22/U, were tested to determine the effect of nuclear exposure rate on insulation conductance, photovoltaic current, rf components of noise, capacitance, and dissipation factor. Measurements were made during radiation exposures at

gamma dose rates ranging from 10^4 to 10^6 r/hr. Of the electrical parameters measured only insulation conductance and photovoltaic current exhibited measurable variation as a function of nuclear exposure rate.

Irradiation tests 5 and 8, reported herein, were the third and fourth in the series of rate effects tests on electrical cables and connectors. In these, the effect of elevated temperature (70°C), combined with nuclear radiation, was investigated for standard and high temperature multiconductor instrumentation cables. Elevated-temperature irradiation tests were also carried out on RG 58/U, RG 141/U and a 5-pin pair of cable connectors.

Section 2
TEST OBJECTIVES

The purpose of irradiation tests 5 and 8 was to determine the effects of radiation rate on the insulation conductance, photovoltaic current, and radio frequency noise for selected coaxial cables, multiconductor cables, and connectors irradiated at 70°C temperature.

Section 3 TEST DESCRIPTION

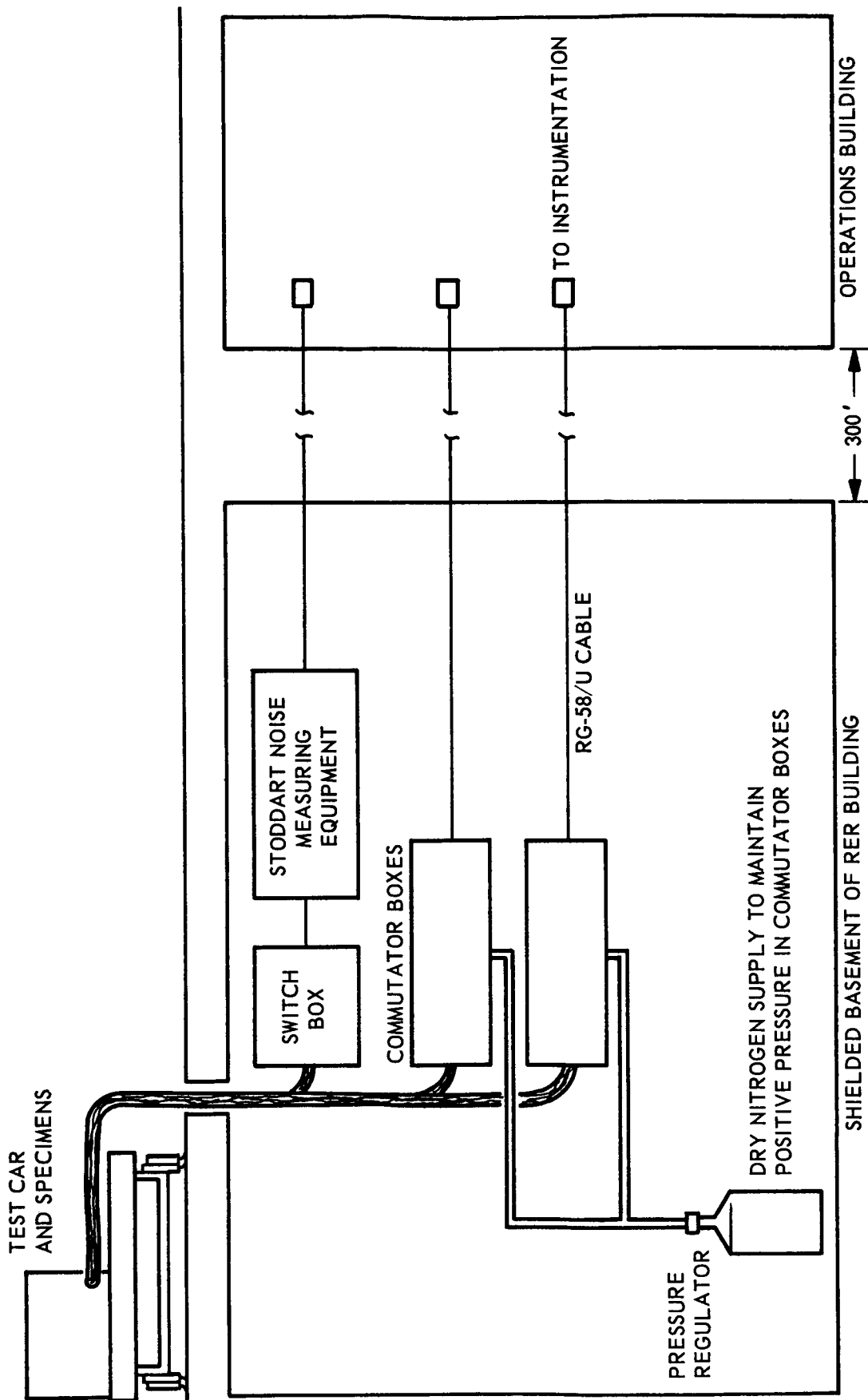
3.1 TEST SPECIMENS

3.1.1 Test 5

The specimens evaluated in test 5 were made from two types of coaxial cable, RG-58C/U and RG-141/U, and two types of four-conductor cable — LMSC Specification MD-324 and Consolidated Wire Corporation CDS-47831. Complete descriptions of the cables, (as provided by the manufacturer) are presented in Table 3-1 and the history of the specimen materials is given in Table 3-2.

Two specimen types were prepared from each cable type. One specimen type was a 60-foot cable length, the other type, a 40-foot. Experiment design was based on exposure of 20 feet of cable to the combined high dose rate and elevated temperature. The additional 40 feet of the 60-foot specimens was required as the initial lead from the test panel on the test car to the instrumentation in the reactor building basement as shown in Figure 3-1. The 40-foot control specimens were mounted between the test panel and the instrumentation in the basement, to permit the determination of any influence on electrical parameter measurements induced by the 40 feet of cable used as the initial lead.

The end of the specimens to be mounted on the test panel were potted in Epon 828 resin cured at room temperature with Epon curing agent V-25. Prior to potting, the outer covering was removed for a distance of 1.5 inches from the ends of the cables (to expose the dielectric) and the conductors were separated.



NSP 6875

Figure 3-1 Instrumentation Cabling

Table 3-1
TEST 5 -- SPECIMEN MANUFACTURER'S SPECIFICATIONS (NOMINAL)

Cable Type	Military Specification	Dielectric Material	Diameter of Dielectric	Center Conductor Material	Diameter of Center Conductor	Shield Material	Jacket Material	Overall Diameter	Impedance (ohms)	Capacity $\mu\text{f}/\text{ft}$	Velocity Propagation (percent)	Maximum Operative Voltage	Operative Temperature Limits
RG-58C/U (coaxial)	MIL-C-17B	Polyethylene	.116	19/.0071 Tinned Copper	.034	Tinned Copper	Black Vinyl Low Temperature Non-Contaminating	.195	50	29.5	65.9	1900	-40°C to +80°C
RG-141/U (coaxial)	MIL-C-17B	Teflon	.116	19 Silver Coated	Not Specified	Silver Coated Copper	Fiberglass	.190	50	28.5	69.5	1900	-55°C to 250°C
MD-324 (4-conductor)	-	Irradiated Polyethylene	-	#24 Stranded Copper	-	Copper	Irradiation Polyethylene	.152	-	-	-	600	-55°C to 135°C
CDS-47831	-	Polyvinyl-chloride	-	#24 Stranded Copper	-	Tinned Copper	Polyvinyl-chloride	.167	-	-	-	600	Not Specified

Table 3-2
TEST 5 -- SPECIMEN HISTORY

Cable Type	Date Acquired	Manufacturer	Production Number	Certificate of Compliance Number	Deviation from Specifications	Applicable MIL-Spec
RG-58C/U	2-15-63	Amphenol	4499-2	1974	None	MIL-C-17B
RG-141/U	2-19-63	ITT Distributor Division	100651*	-	None	MIL-C-17B
MD-324	2-19-63	Raychem Corp.	J6-1-14-63-7	10124	None	MD-324 and LAC 01-4006A
CDS-47831	3-1-63	Consolidated Wire Corp.	281-749*	-	None	None

*Invoice Number

Two sets of specimens of each type of cable were prepared. One set was for irradiation tests and the other was for control. The number and type of specimens of each cable type for control and for irradiation tests are specified in Table 3-3.

3.1.2 Test 8

The specimens evaluated in test 8 were made from one type of twisted pair cable (RT24(19)ST 2RO/9-0), one type of 4-conductor cable (PSC-C-39001-4-24ST), and one type of connector (PT00P-14-5 S, socket, and PT06P-14-6 P plug). Complete descriptions of the cables and connectors (as provided by the manufacturer) are presented in Table 3-4 and the history of the specimen materials, in Table 3-5. The entries for the MD-324 cable are included in these tables since this cable was used in connection with the type-PT connector test.

Two specimen types were prepared from the RT and PSC cables. One specimen type was a 60-foot cable length, the other type, a 40-foot. Experiment design was based on exposure of 20 feet of cable to the combined high dose rate and elevated temperature. The additional 40 feet of the 60-foot specimens was required as the initial lead from the test panel on the test car to the instrumentation in the reactor building basement as shown in Figure 3-1. The 40-foot control specimens were mounted between the test panel and the instrumentation in the basement, to permit the determination of any influence on electrical parameter measurements induced by the 40 feet of cable used as the initial lead.

The PT connector specimens were prepared as follows: Two 45-foot lengths of MD-324 cable were cut. Five sets of connectors were then placed in series approximately six inches apart along the last 30 inches of each of these 45-foot lengths. This was done by cutting the cable at appropriate points and soldering the cable shield to the shell and one of the connector pins and one of the cable conductors to each of the other four connector pins. After

Table 3-3
TEST 5 -- SPECIMEN SUMMARY

Cable Type	Number of Specimens	Length Feet	Number of Control Specimens	Total Length of Control Specimens Feet	Total Number of Specimens
ELEVATED TEMPERATURE CONTROL (REL)					
RG-58C/U	3	60'	1	40'	4
RG-141/U	3	60'	1	40'	4
MD-324	3	60'	1	40'	4
CDS-47831	3	60'	1	40'	4
IRRADIATION AND ELEVATED TEMPERATURE (REF)					
RG-58C/U	4	60'	1	40'	5
RG-141/U	4	60'	1	40'	5
MD-324	3	60'	1	40'	4
CDS-47831	3	60'	1	40'	4

Table 3-4
TEST 8 -- SPECIMEN MANUFACTURER'S SPECIFICATIONS (NOMINAL)

Cable Type	Military Specifications	Dielectric Material	Diameter Dielectric	Center Conductor Material	Diameter of Center Conductor	Shield Material	Jacket Material	Overall Diameter	Maximum Operative Voltage	Operative Temperature Limits
PSC-C-39001-4-24ST (4-Conductor)	-	Silica-Glass	-	#24 Stranded Nickel-Clad Copper	-	Stainless Steel	Stainless Steel	.350, .460 and .480 in.	600	1000°F
MD-324 (4-Conductor)	-	Irradiated Polyethylene	-	#24 Stranded Copper	-	Copper	Irradiated Polyethylene	.152 in.	600	-55°C to +135°C
RT24(19)ST2RO/9-0 (2-Conductor, twisted pair)	-	Irradiated Polyethylene	-	19/36 #24 Stranded Tinned Copper	-	Tin Plated Copper	Irradiated Polyethylene	.135 in.	600	-55°C to +135°C
PT00P-14-5S and PT06P-14-5P (Connectors)	MIL-C-26482	Neoprene	.657	-	-	-	-	1.15 in.	1500	-55°C to +125°C

Table 3-5
TEST 8 -- SPECIMEN HISTORY

Cable Type	Date Acquired	Manufacturer	Production Number	Certificate of Compliance Number	Deviation from Specification	Applicable MIL-Spec.
PSC-C-39001-4-24ST	3-27-63	Physical Science Corporation	4358 4888 4909	Dtd. 1-31-63 0450 0397	Different Outside Diameters Coloration	None
MD-324	2-19-63	Raychem Corp.	J6-1-14-63-7	10124	None	MD-324 and LAC 01-4006A
RT24(19)ST2RO/9-0	3-27-63	Raychem Corp.	I6-9-19-62-10	1220E	None	None
PT00P-14-5 S PT06P-14-5 P	3-23-63	Bendix Corp.	40175FC*	Curwork Corp. 3-23-63	None	MIL-C-26482

*Invoice Number

soldering, the connectors were potted with 3M#XR5038 potting compound (an epoxy resin) mixed according to manufacturer's directions and cured at room temperature. The connectors were then mounted horizontally on the test panel and the other end of the MD-324 cable was connected to the instrumentation in the reactor building basement. An additional 45-foot length of MD-324 cable, without connectors, was similarly mounted to permit correction for any influence the connecting cable might exert on the connector parameter measurements.

The ends of the specimens to be mounted on the test panel were potted in Epon 828 resin, and cured at room temperature with Epon curing agent V-25. Prior to potting, the outer covering was removed for a distance of 1.5 inches from the ends of the cables (to expose the dielectric) and the conductors were separated.

Two sets of specimens of each type of cable were prepared. One set was for irradiation tests and the other was for control testing. The control specimens for the PT type connector were also used to test for the effect of the 3M#XR5038 potting compound on photovoltaic current and leakage conductance at ambient temperature. The number and type of specimens of each cable type for control and for irradiation tests are specified in Table 3-6.

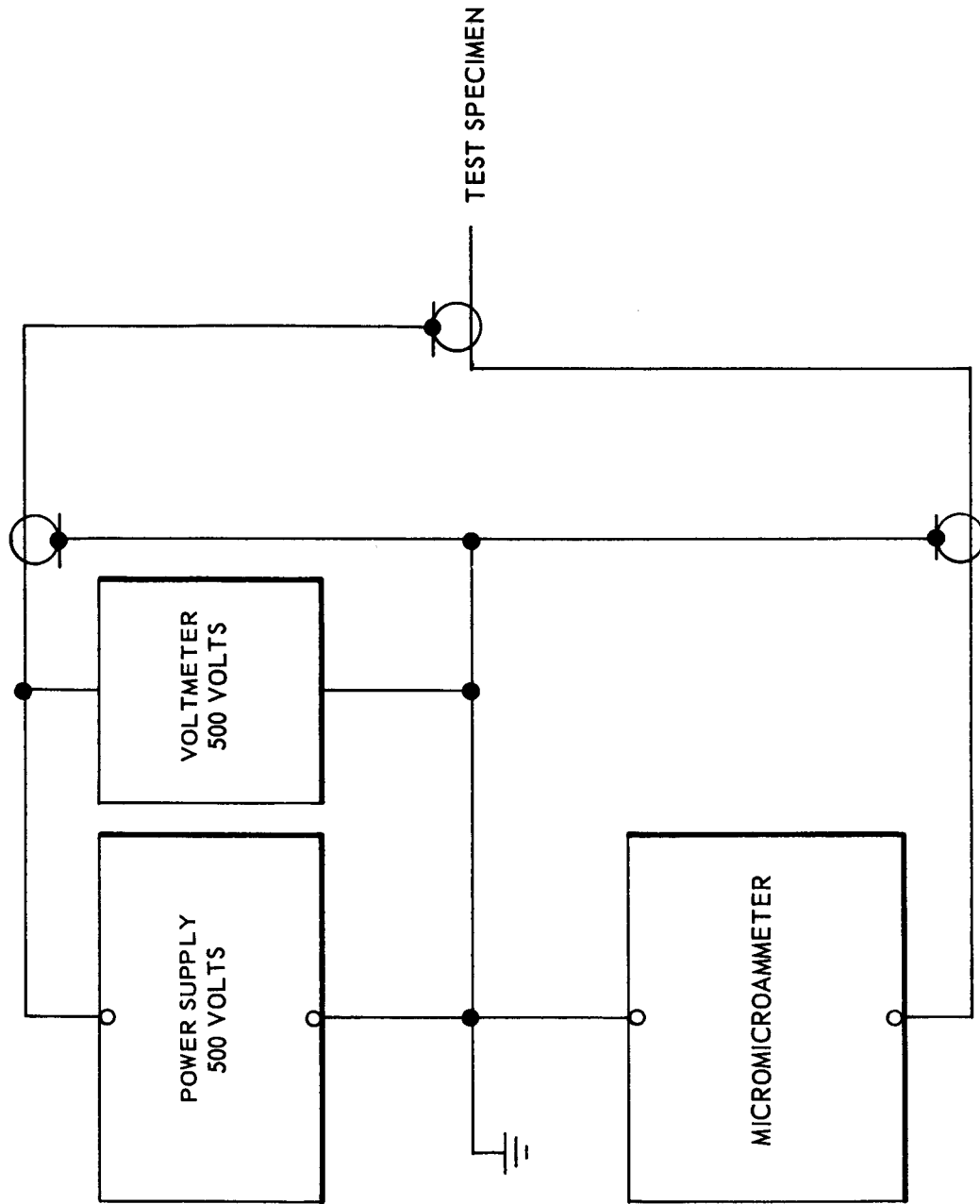
3.2 TEST EQUIPMENT

3.2.1 Electrical

Detailed descriptions of the measurement systems are given in Ref. 2. In summary the instrumentation cabling arrangement is shown in Figure 3-1 and block diagrams of the electrical test instrumentation are presented in Figures 3-2 and 3-3. The irradiation test specimens were located on a test car adjacent to the reactor and were approximately 38 cable feet from the commutation boxes. Each of these boxes contained a stepping switch, remotely controlled from the operations building, which was connected by

Table 3-6
TEST 8 -- SPECIMEN SUMMARY

Cable Type	Number of Specimens	Length (feet)	Number of Control Specimens	Total Length of Control Specimens (feet)	Total Number of Specimens
ELEVATED TEMPERATURE CONTROL (REL)					
PSC-C-39001-2-24ST	3	60'	1	40'	4
RT24(19)2RO/9-0	3	60'	1	40'	4
MD-324 With 5 PT Connectors in Series	2	45'	1 (Without Connector Specimens)	45'	3
IRRADIATION AND ELEVATED TEMPERATURE (REF)					
PSC-C-39001-4-24ST	3	60'	1	40'	4
RT24(19)2RO/9-0	3	60'	1	40'	4
MD-324 With 5 PT Connectors in Series	2	45'	1 (Without Connector Specimens)	45'	3



NSP 6876

Figure 3-2 Insulation Conductance and Photovoltaic Current Measurement

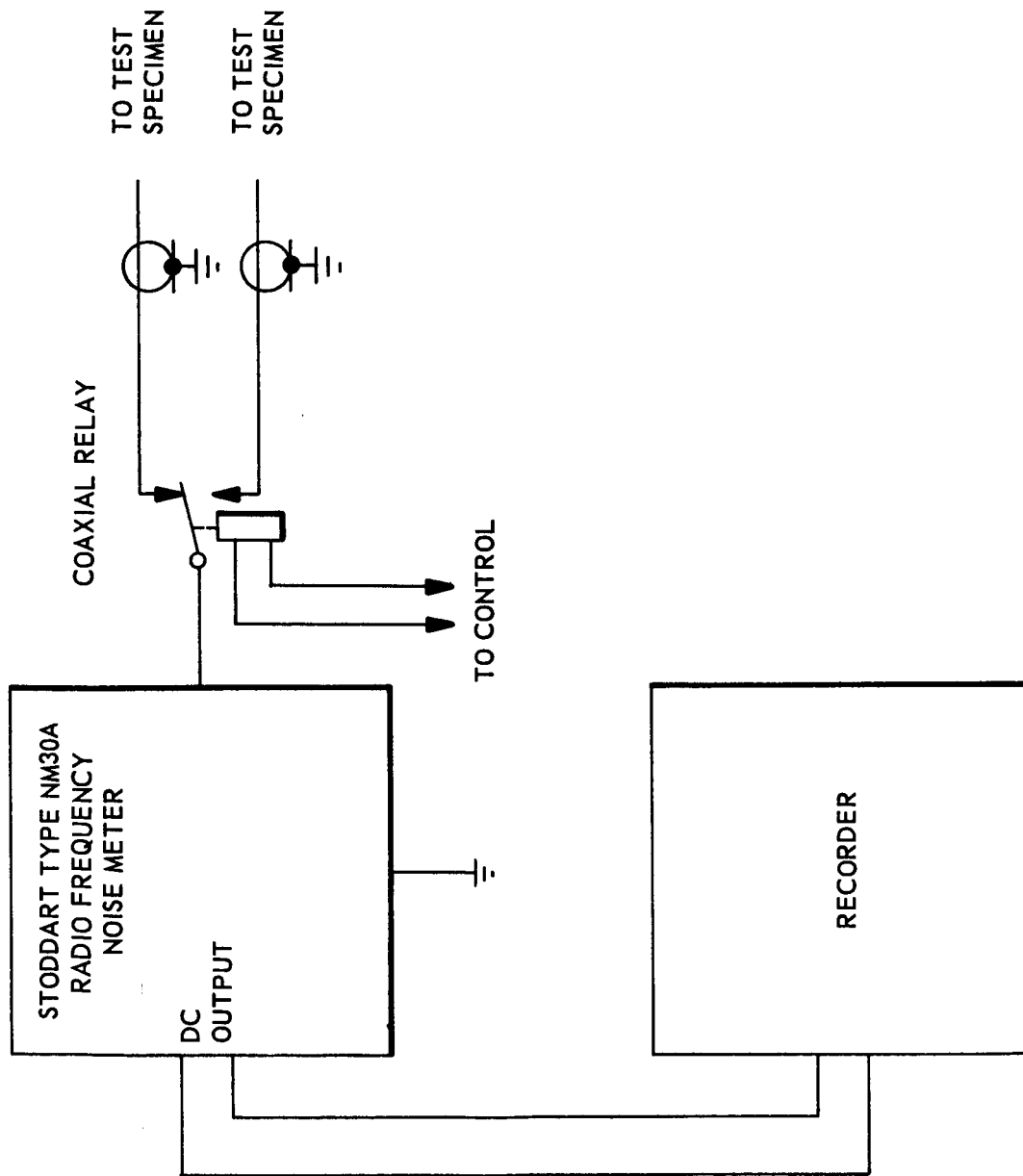


Figure 3-3 R-F Noise Measurement

NSP 6877

installed instrumentation cables to the measurement system in the operations building. A dry nitrogen atmosphere was maintained in the commutation boxes to prevent humidity variations that would affect resistance measurements.

The insulation conductance was measured by the system shown in Figure 3-2. A bias voltage of -500 volts dc was provided, and the resulting current flow was measured. A guard shield was used for the installed instrumentation cables between the operations area and the reactor building; this arrangement allowed measurement of the insulation conductance without the shunting conductance of the long 300-ft instrumentation cables. Positive polarity of the recorded data is defined to correspond to current flowing from the center conductor to the shield inside the cable. A pen recorder was used in the current monitoring system as a visual means of observing that the current had reached equilibrium before the measurement was made.

The instrumentation described above for conductance measurements was also used to measure the photovoltaic current except that the power source was short-circuited to provide a circuit for the current flow.

The system used for measuring the 400-mc component of generated noise is shown in Figure 3-3. Two coaxial cables, RG-58C/U and RG-141/U, were permanently connected to a coaxial switch that permitted either cable to be connected to the system. The Stoddart noise meter had a bandwidth of 150 kc and an internal noise level of about 10 db. The meter was located about 38 cable feet from the test specimens and the pen recorder indicated the noise level measured by the instrument. The specimens were not loaded at the terminals.

3.2.2 Nuclear Measurements

Lockheed Model 505 ionization chambers were used to monitor the gamma dose rates to which the cables were exposed. The Model 505 is a graphite-walled, CO₂-filled chamber with a sensitive volume of 4 cm³. Each chamber was calibrated prior to the irradiation test in a known kilocurie Co⁶⁰ source field.

Neutron activation foils and a Th^{232} fission chamber were used to measure neutron flux for the fast and thermal energy regions. The Th^{232} fission chamber provided an auxiliary measurement that was used to evaluate the counting results of Th^{232} foils. Foil materials and reactions that were utilized are tabulated below, and the methods used for evaluating the foil activity are described in Ref. 3.

Foil Material and Reaction	Effective Threshold Cross Section* (Barns)	Effective Threshold Energy* (Mev)
$\text{Th}^{232}(\text{n}, \text{f})\text{F. P.}$	0.15	1.7
$\text{S}^{32}(\text{n}, \text{p})\text{P}^{32}$	0.30	2.9
$\text{Ni}^{58}(\text{n}, \text{p})\text{Co}^{58}$	1.23	5.0
$\text{Mg}^{24}(\text{n}, \text{p})\text{Na}^{24}$	0.048	6.3
$\text{Al}^{27}(\text{n}, \alpha)\text{Na}^{24}$	0.11	8.1
$\text{Co}^{59}(\text{n}, \gamma)\text{Co}^{60}$	36.3**	Thermal

* Effective threshold cross sections and the corresponding effective threshold energies are calculated on the basis of a fission spectrum.

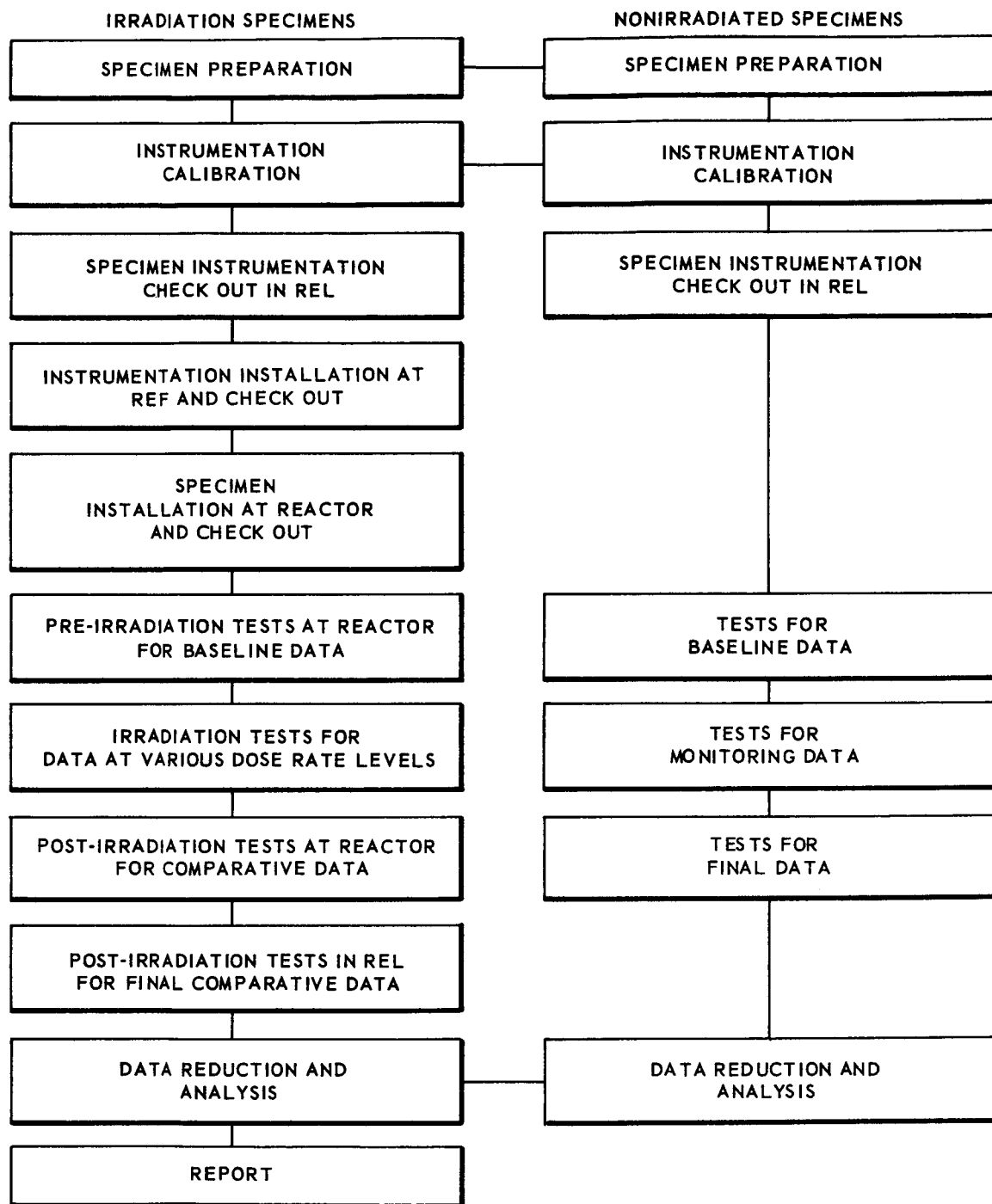
** 2200 m/s cross section

3.3 TEST PROCEDURE

A detailed description of the test procedure is included in Ref. 2. The test flow diagram, Figure 3-4, gives the sequence of the major steps of the test program.

3.3.1 Controls

As specified in Section 3.1.2, two sets of specimens mounted on separate test panels were tested. One set, used as non-irradiated controls was



NSP 6878

Figure 3-4 Test Flow Diagram

subjected to the same temperature for the same periods, and to the same tests as the irradiated specimens. The other set was irradiated. As shown in Tables 3-3 and 3-6, one 40-foot specimen of each cable was installed between the commutation boxes and the test panels to permit control measurements on the effect of this portion of the 60-foot specimens on the electrical parameters measured. Also, a portion of a 45-foot length of MD-324 cable was installed on the test panel and its remainder was run from the test panel to the commutation boxes to permit control measurements on the effect of the MD-324 cable on the connector specimen measurements.

3.3.2 Temperature

Both the control and irradiation tests were conducted with 20-foot sections of the total specimen lengths mounted on the test panel. Each connector specimen consisted of five connectors in series mounted horizontally across the test panel. Test specimens were held at $70 \pm 3^{\circ}\text{C}$ ($158 \pm 5^{\circ}\text{F}$). Temperature transducers were mounted at five points on each test panel and the temperature was continuously monitored and recorded during the tests.

3.3.3 Electrical Measurements

The insulation conductance and photovoltaic current were measured:

A. On the control specimens

- Immediately after reaching the test temperature (70°C)
- After the same elapsed time at 70°C as the irradiated specimens when tested
- On the PT-type connector specimens only, at ambient temperature, before and after potting the connectors with 3M#XR5038

B. On the irradiated specimens

- Before irradiation, at the REL (Radiation Effects Laboratory) without the 300 feet of extension cable at ambient temperature and at 70°C .
- Before irradiation at the REF (the reactor site) with the complete instrumentation system to be used during the irradiation tests.

- During irradiation at each of the following nominal gamma dose rates: 10^4 , 10^5 , 5×10^5 , 10^6 , and 2×10^6 r/hr
- Immediately after irradiation at the REF
- After irradiation at the REL at 70°C and at ambient temperature

3.3.4 Nuclear Measurements

Radiation rates at each measurement location (shown in Figures 3-5 and 3-6) were monitored at the power levels corresponding to nominal gamma dose rates of 10^4 , 10^5 , 5×10^5 , 10^6 and 2×10^6 r/hr. The dose rate, measured by ionization chamber 7, was taken as a reference for adjusting the reactor power to obtain the specified gamma radiation levels.

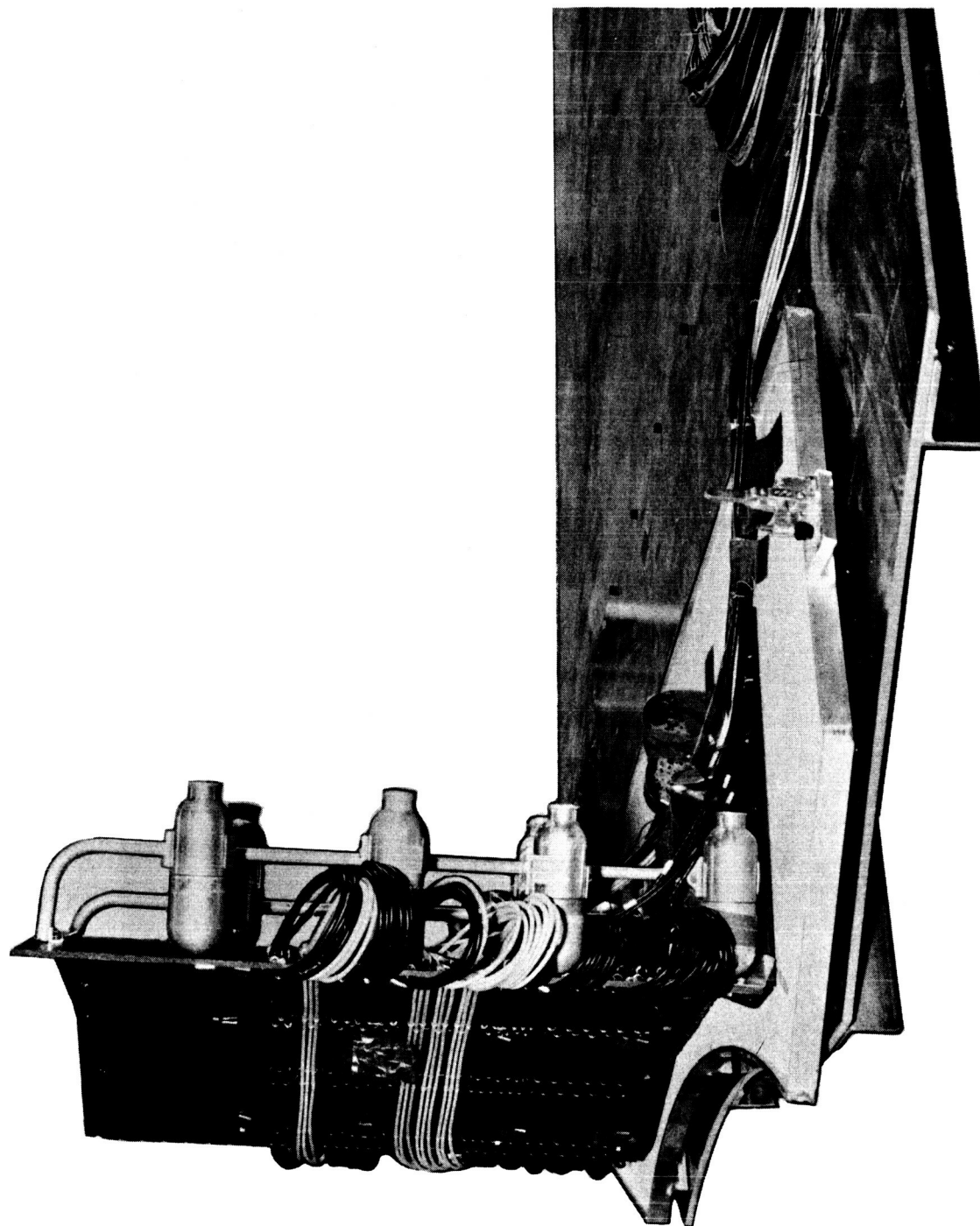
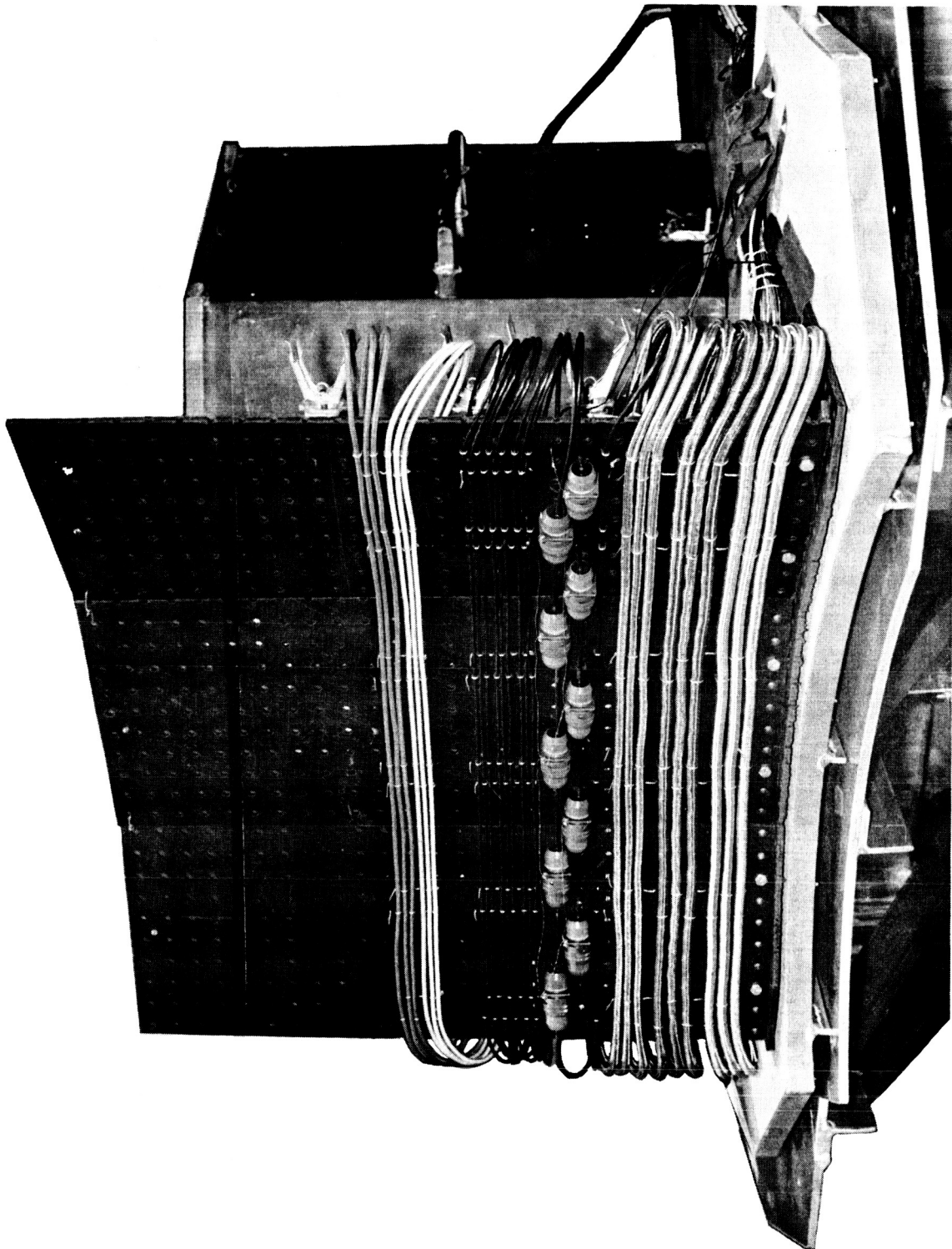


Figure 3-5 Mounting for Cable Specimens

NSP 6879



NSP 6880

Figure 3-6 Mounting for Cable and Connector Specimens

Section 4 RESULTS

4.1 ENVIRONMENTAL DATA

4.1.1 Temperature

Figure 4-1 is a temperature history of irradiation 5; Figure 4-2 of irradiation 8. Unless otherwise noted, data for both control and irradiated specimens were taken at 70°C. Test 5 accumulated 169 hours; test 8, 106.5 hours.

4.1.2 Radiation Environment

Gamma dose rate isoplots of the test panels for irradiations 5 and 8 are shown in Figures 4-3 and 4-4, respectively. The values appearing on the plot have been normalized as factors of the actual dose rates. Tables 4-1 and 4-2 tabulate the ratio of the average actual radiation level for each specimen to the actual radiation level for the test panel. Thus, the average actual gamma dose rate or neutron flux for each specimen may be determined by multiplying the listed actual gamma dose rate or respective neutron flux by the listed radiation rate ratio.

A fast neutron spectrum, measured near the center of the test panel with threshold foils, is shown in Figures 4-5 and 4-6. No gamma energy spectra were measured during the test since it is not feasible to measure gamma spectra in an intense radiation field. Gamma leakage-spectra measurements about the RER, made previously during low-power operation, are shown in Figure 4-7.

4.1.3 Applied Voltage

All photo current measurements were obtained with zero voltage, while conductance measurements were made with a 500-vdc potential.

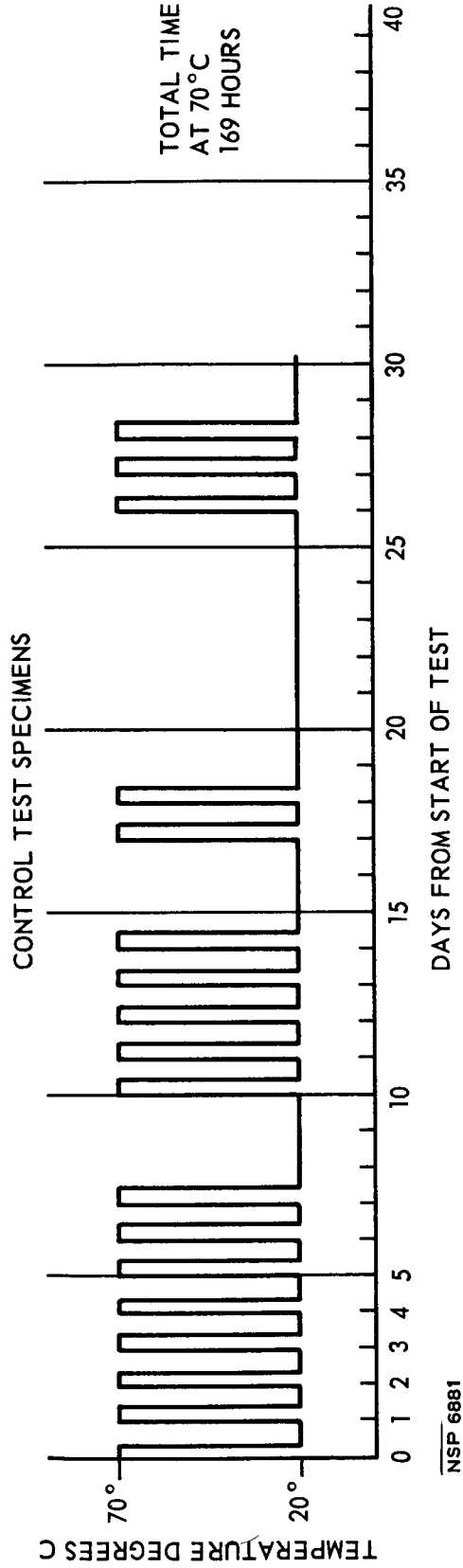
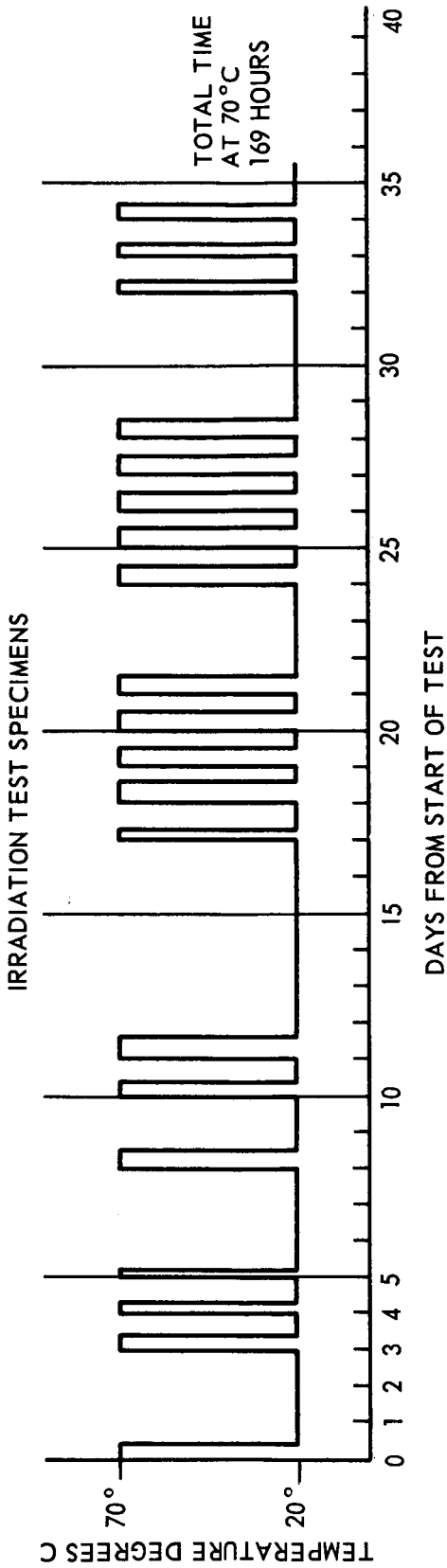
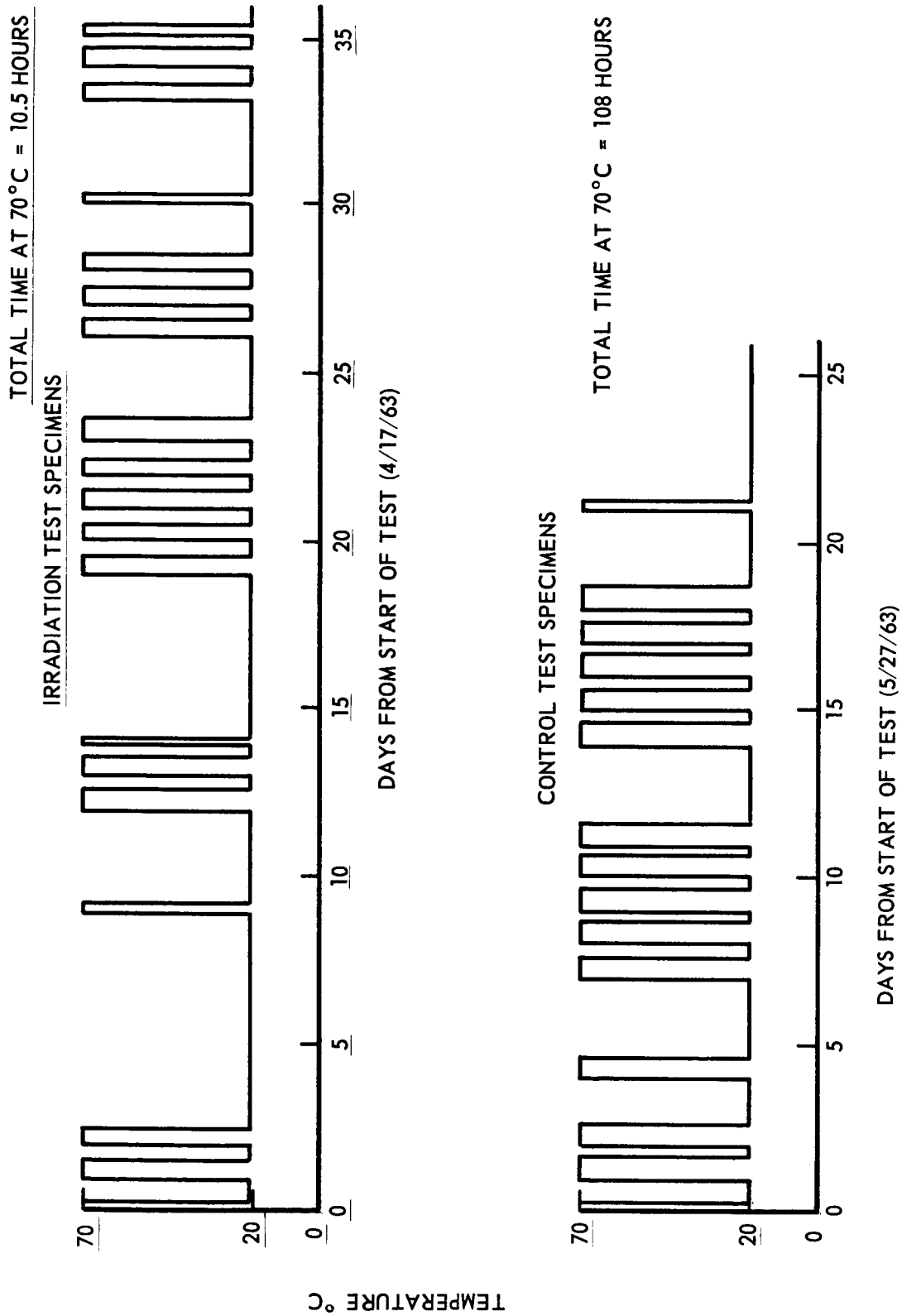


Figure 4-1 Irradiation 5 -- Temperature History of Test Specimens



NSP 6882

Figure 4-2 Irradiation 8 -- Temperature History of Test Specimens

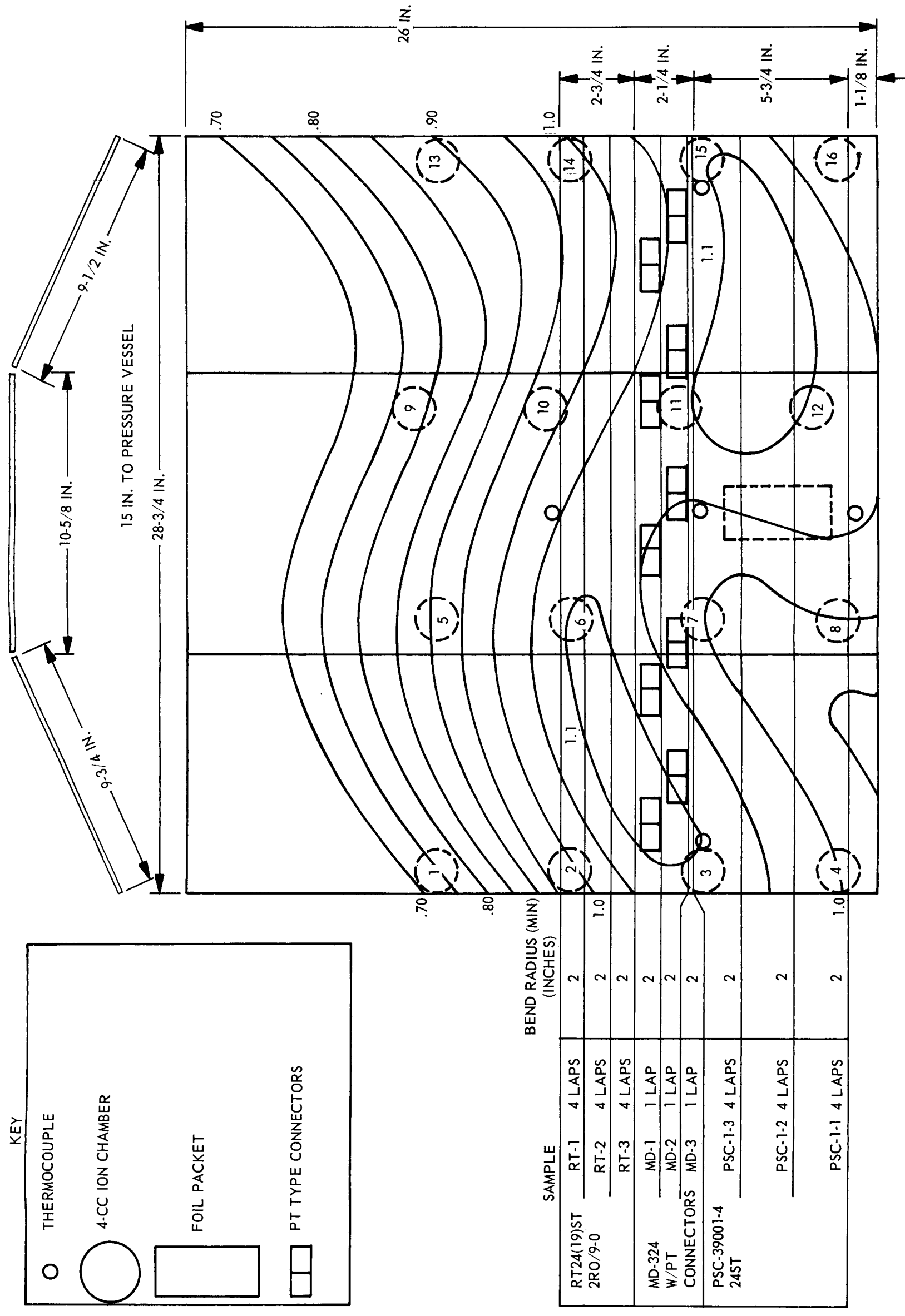
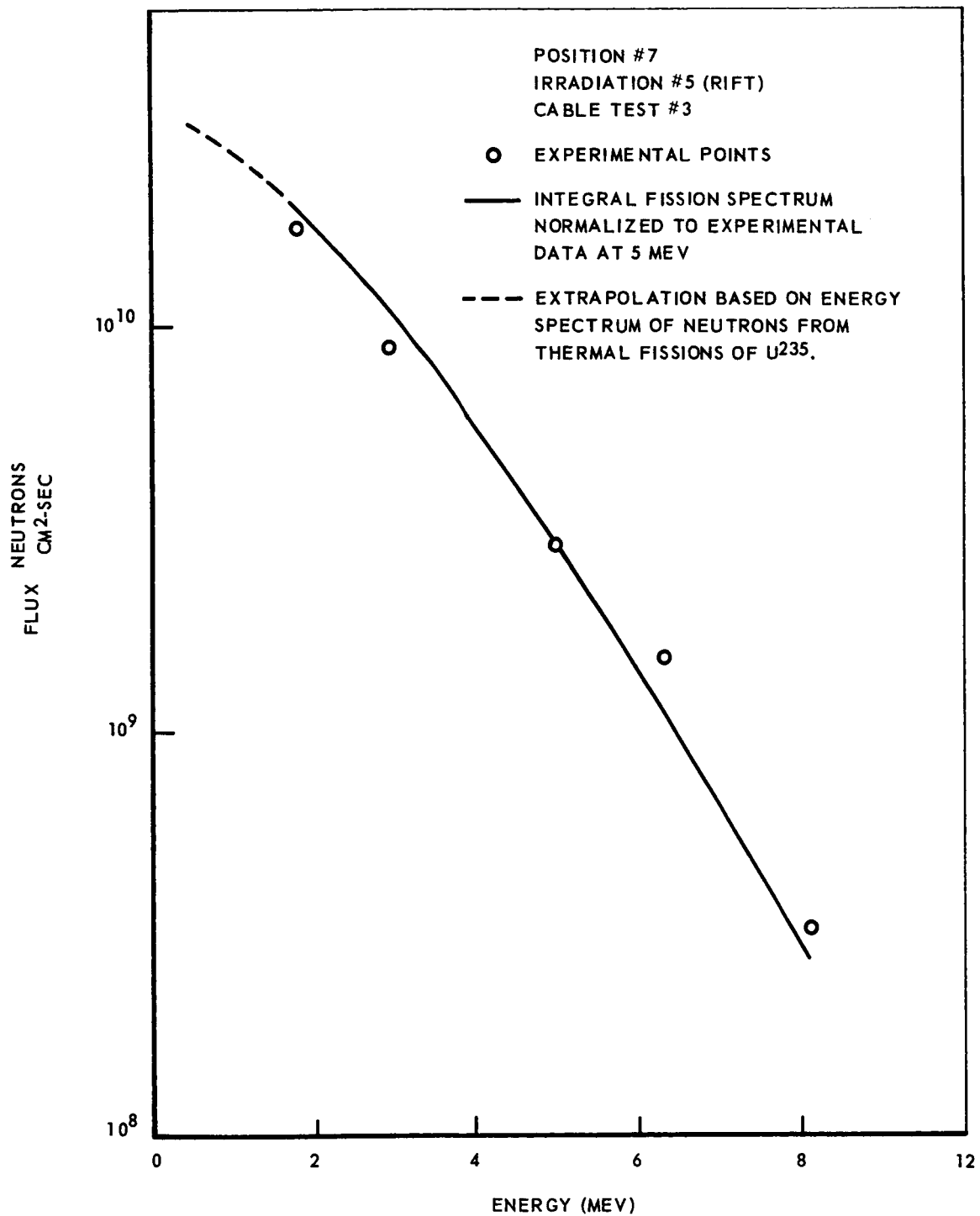


Figure 4-4 Irradiation 8 -- Test Panel Plan with Gamma Dose-Rate Isodose

Table 4-1
TEST 5--RADIATION ENVIRONMENT

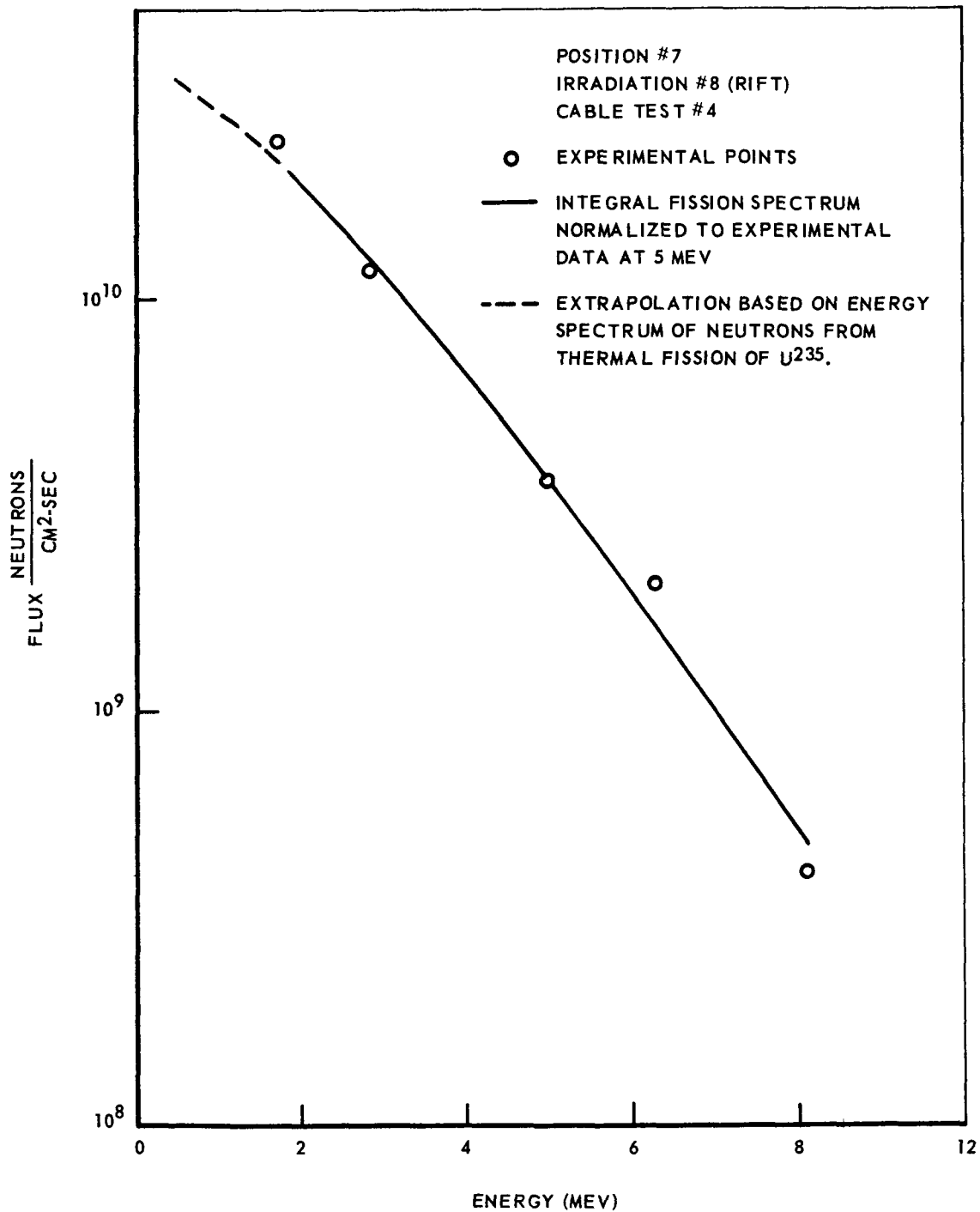
NOMINAL RADIATION LEVELS				
Gamma r/hr	Neutrons >0.5 Mev	n/cm ² /Sec Thermal		
10 ⁴	1.6 x 10 ⁸	1.6 x 10 ⁸		
10 ⁵	1.6 x 10 ⁹	1.6 x 10 ⁹		
5 x 10 ⁵	8.0 x 10 ⁹	8.0 x 10 ⁹		
10 ⁶	1.6 x 10 ¹⁰	1.65 x 10 ¹⁰		
2 x 10 ⁶	3.2 x 10 ¹⁰	3.3 x 10 ¹⁰		
Average Accumulated Exposure				
Specimen Number	Radiation Rate Ratio*	Gamma r	Neutrons n/cm ²	
			>0.5 Mev	Thermal
RG-58-1 -2 -3 -5	.987	3.16 x 10 ⁷	1.68 x 10 ¹⁵	1.78 x 10 ¹⁵
	.963	3.08 x 10 ⁷	1.63 x 10 ¹⁵	1.73 x 10 ¹⁵
	.933	2.98 x 10 ⁷	1.58 x 10 ¹⁵	1.66 x 10 ¹⁵
	.881	2.82 x 10 ⁷	1.50 x 10 ¹⁵	1.58 x 10 ¹⁵
RG-141-1 -2 -3 -5	1.053	3.37 x 10 ⁷	1.79 x 10 ¹⁵	1.90 x 10 ¹⁵
	1.038	3.32 x 10 ⁷	1.77 x 10 ¹⁵	1.87 x 10 ¹⁵
	1.013	3.24 x 10 ⁷	1.72 x 10 ¹⁵	1.82 x 10 ¹⁵
	.861	2.75 x 10 ⁷	1.46 x 10 ¹⁵	1.55 x 10 ¹⁵
MD-324-1 -2 -3	1.108	3.52 x 10 ⁷	1.87 x 10 ¹⁵	1.98 x 10 ¹⁵
	1.096	3.51 x 10 ⁷	1.86 x 10 ¹⁵	1.97 x 10 ¹⁵
	1.076	3.44 x 10 ⁷	1.81 x 10 ¹⁵	1.94 x 10 ¹⁵
PVC-1 -2 -3	1.139	3.65 x 10 ⁷	1.94 x 10 ¹⁵	2.05 x 10 ¹⁵
	1.138	3.64 x 10 ⁷	1.93 x 10 ¹⁵	2.05 x 10 ¹⁵
	1.128	3.61 x 10 ⁷	1.91 x 10 ¹⁵	2.03 x 10 ¹⁵

*Radiation Rate Ratio = $\frac{\text{Actual Radiation Level}}{\text{Nominal Radiation Level}}$



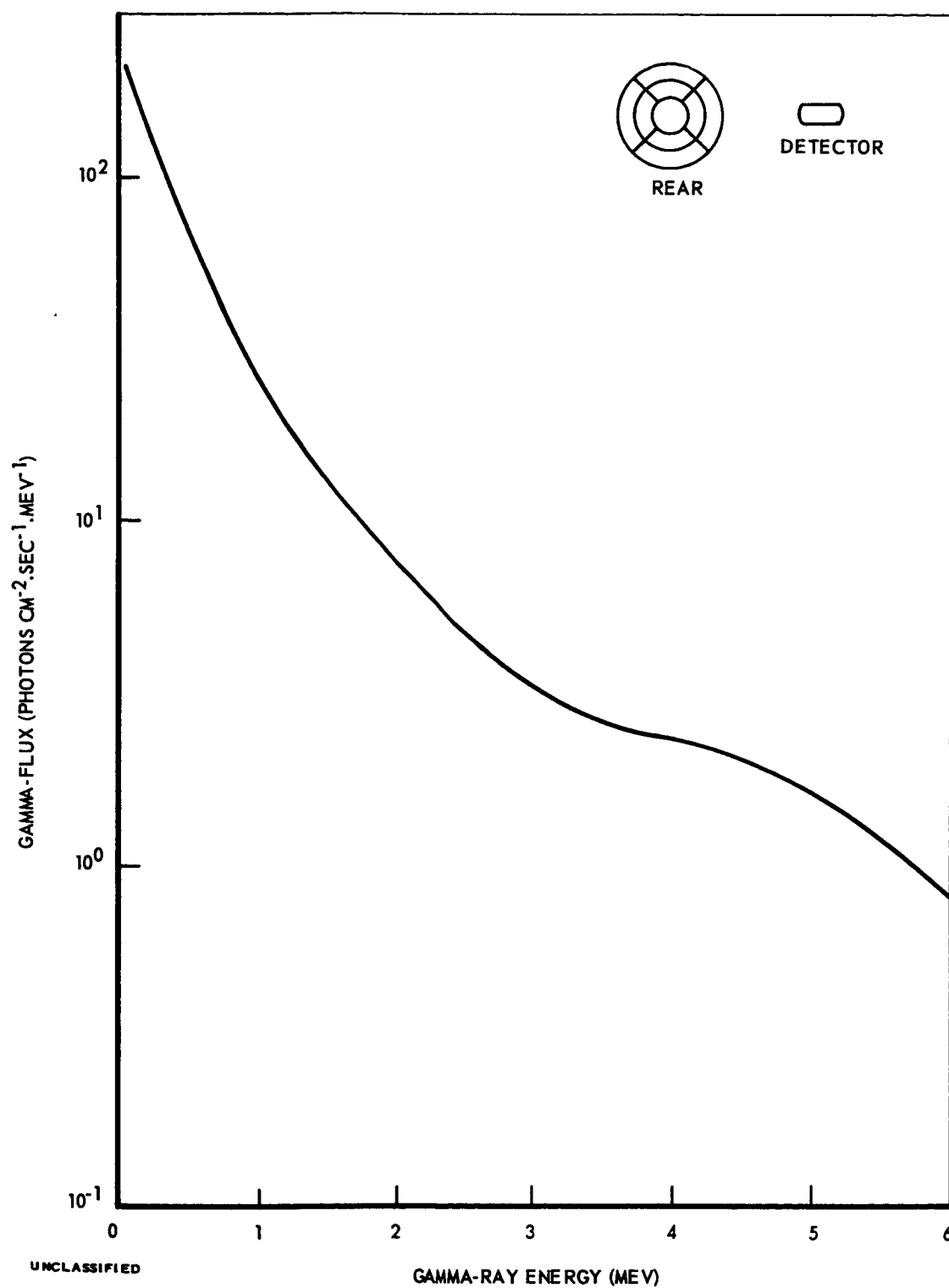
NSP 6885

Figure 4-5 Irradiation 5 -- Fast Neutron Flux above
Effective Threshold Energy



NSP 6886

Figure 4-6 Irradiation 8 -- Fast Neutron Flux above
Effective Threshold Energy



NSP 6887

Figure 4-7 Gamma-Ray Energy Spectrum of the RER

4.2 DATA REDUCTION

Data were reduced on the basis of the equations to be discussed. For purposes of dc circuit analysis, an electrical cable in a radiation field can be considered as a network of apparent conductances and apparent current generators. The data from these tests were processed to yield the values of these conductances and current generators in the networks that are equivalent to coaxial two-conductor and four-conductor cables, and five-pin connectors.

4.2.1 Coaxial Cable Measurements

The equations derived in Ref. 5 for two-terminal cable are:

$$(1) \quad G_s = \frac{1}{L \times E} \left[(I_S - I_{SO}) - (I_C - I_{CO}) \right]$$

$$(2) \quad i_S = \frac{1}{L} (I_{SO} - I_{CO})$$

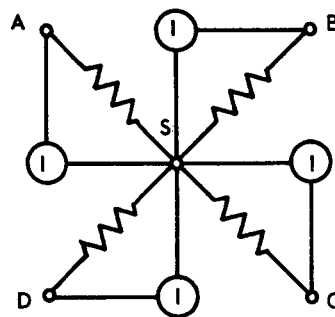
where

- G_s = conductance per lineal foot
- i_S = photovoltaic current per lineal foot
- E = applied voltage, 500 vdc
- I_S = measured current with 500 volts applied to full test sample
- I_{SO} = measured current with power source shorted; from full test sample
- I_C = measured current with 500 volts applied to control length sample (#4)
- I_{CO} = measured current with power source shorted; from control length test sample (#4)
- L = irradiated length of test sample (20 feet).

4.2.2 Four-Conductor Cable Measurements

The four-conductor cable can be connected into two-terminal configurations involving all conductors and the shield. The notation for these configurations employs a slash. For example, SAD/BC means that Conductors B and C are connected together to form one terminal of the system and Conductors A and D and the shield form the other terminal. During this test, the configurations S/ABCD, SAD/BC and SAC/BD were used for measurement of the parameters.

Conductivity Calculations. Although there are apparently ten possible paths of conductance in the four-cable configuration, the experimental data indicates that only four paths are of significance. Therefore, the equivalent circuit based on the experimental data is as follows.



From the circuit shown above, these equations were written:

$$(3) \quad G_{S/ABCD} = 4 G_E$$

$$(4) \quad G_{SAD/BC} = 2 G_E$$

$$(5) \quad G_{SAC/BD} = 2 G_E$$

One value of G_E was derived from Equation (3), and a second value was derived from the sum of Equations (4) and (5).

Based on the above model, three equations relate the apparent currents to the measured two-terminal currents. The measured values are treated in a manner similar to that of Section 4.2.1, viz, $I_S \approx I_{S/ABCD}$ will be calculated from Equation (2). The three equations are:

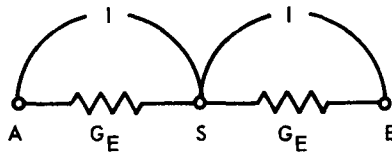
$$(6) \quad I_{S/ABCD} \approx 4 I_E$$

$$(7) \quad I_{SAD/BC} \approx 2 I_E$$

$$(8) \quad I_{SAC/BD} \approx 2 I_E$$

4.2.3 Two-Conductor Cable Measurements

From the previous results, the two-conductor cable equivalent circuit may be represented as follows:



Current measurements were made on this cable by the two-terminal method described in Section 4.2.1. Currents and conductances will be identified by the same subscript system as used for the four-conductor cable.

Conductance Calculations. From the above circuit these equations are written with G_E being the conductance between the shield and conductor:

$$(9) \quad G_{S/AB} \approx 2 G_E$$

$$(10) \quad G_{SA/B} \approx G_E$$

$$(11) \quad G_{SB/A} \approx G_E$$

Photovoltaic Current Calculations. I_E is defined as the mean current generated from each conductor to the shield.

Three equations relate these apparent currents to the measured two-terminal currents. The measured values are treated in a manner similar to that of Section 4.2.1, viz, $I_S = I_{S/AB}$ will be calculated from Equation (2). The three equations are:

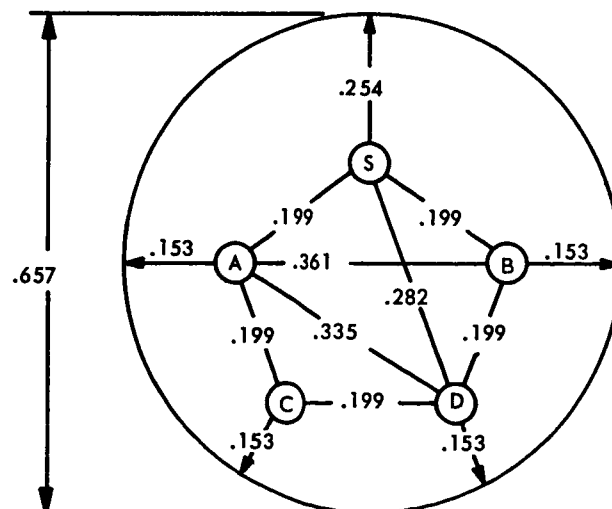
$$(12) \quad I_{S/AB} = 2 I_E$$

$$(13) \quad I_{SA/B} = I_E$$

$$(14) \quad I_{SB/A} = I_E$$

4.2.4 Five-Pin Connector Measurements

A dimensioned cross-section of the PT type connector showing the relative pin positions of the shield and conductors of the interconnecting MD-324 cable is shown below:



Measurements on the connector samples were made in a manner identical to those made on the four-conductor cable.

Conductivity Calculations. Total conductivities were calculated from Equation (1) of Section 4.2.1, substituting the number 5 for L in the equation, since five connectors were involved rather than a length of cable.

Since the 5th pin of the connector is grounded to the shield, the equivalent electrical circuit of the PT connector is assumed to be the same as that of the four conductor cable model.

The conductance of this circuit may be written:

$$(15) \quad G_{S/ABCD} = 4 G_E$$

$$(16) \quad G_{SAD/BC} = 2 G_E$$

$$(17) \quad G_{XAC/BD} = 2 G_E$$

As is the case with 4-conductor cables, the experimental data supports the assumption of these three equations. This is reasonable because the integral of conductance from pin to shell is much greater than that between pins.

Photovoltaic Current Calculations. Total photovoltaic currents for each of the three two-terminal measurement configurations were calculated by Equation (2) of Paragraph 4.2.1 substituting the number "5" for "L" in the equation since five connectors were involved rather than a length of cable.

Based on the above equivalent circuit the photovoltaic current can be calculated from:

$$(18) \quad I_{S/ABCD} = 4 I_E$$

$$(19) \quad I_{SAD/BC} = 2 I_E$$

$$(20) \quad I_{SAC/BD} = 2 I_E$$

Again, the experimental data justifies the simplification of the equivalent circuit; and, as the currents due to charges on the shell and one pin are much greater than those due to charges on two pins, the currents between pin and shell are of greatest significance. This fact is due, at least in part, to the large shell area whereon charges collect.

4.3 EXPERIMENTAL RESULTS

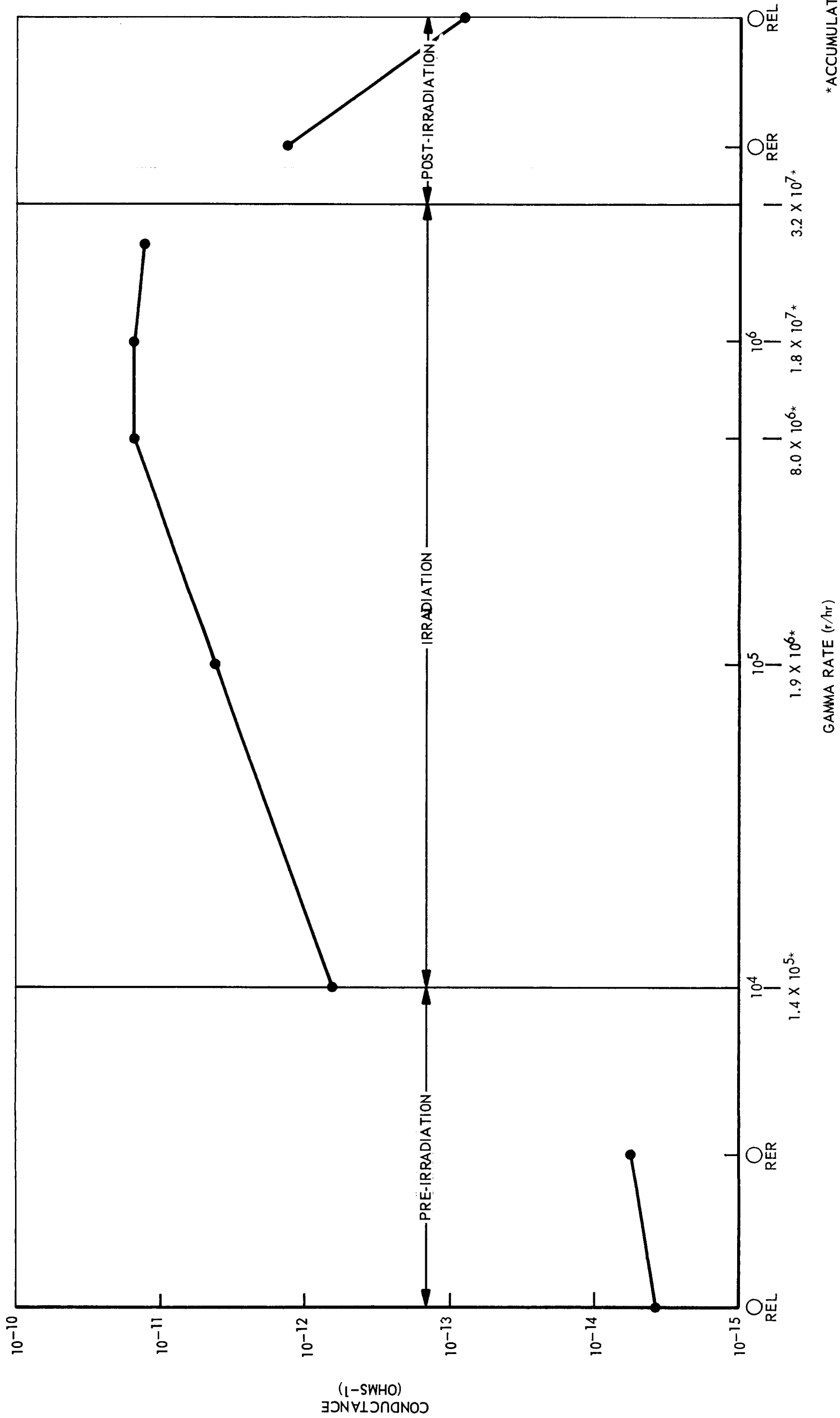
4.3.1 Coaxial Cables—RG 58C/U and RG-141

Figures 4-8, 4-9 and 4-10 present the data which resulted from the coaxial cable measurements. Figures 4-8 and 4-9 present the conductance as defined by equation (1) of paragraph 4.2.1. These data show close agreement between the specimens tested.

The control samples at elevated temperature, did not show any ageing effect during the duration of the experiment. The pre- and post-irradiation measurements are plotted on the graph.

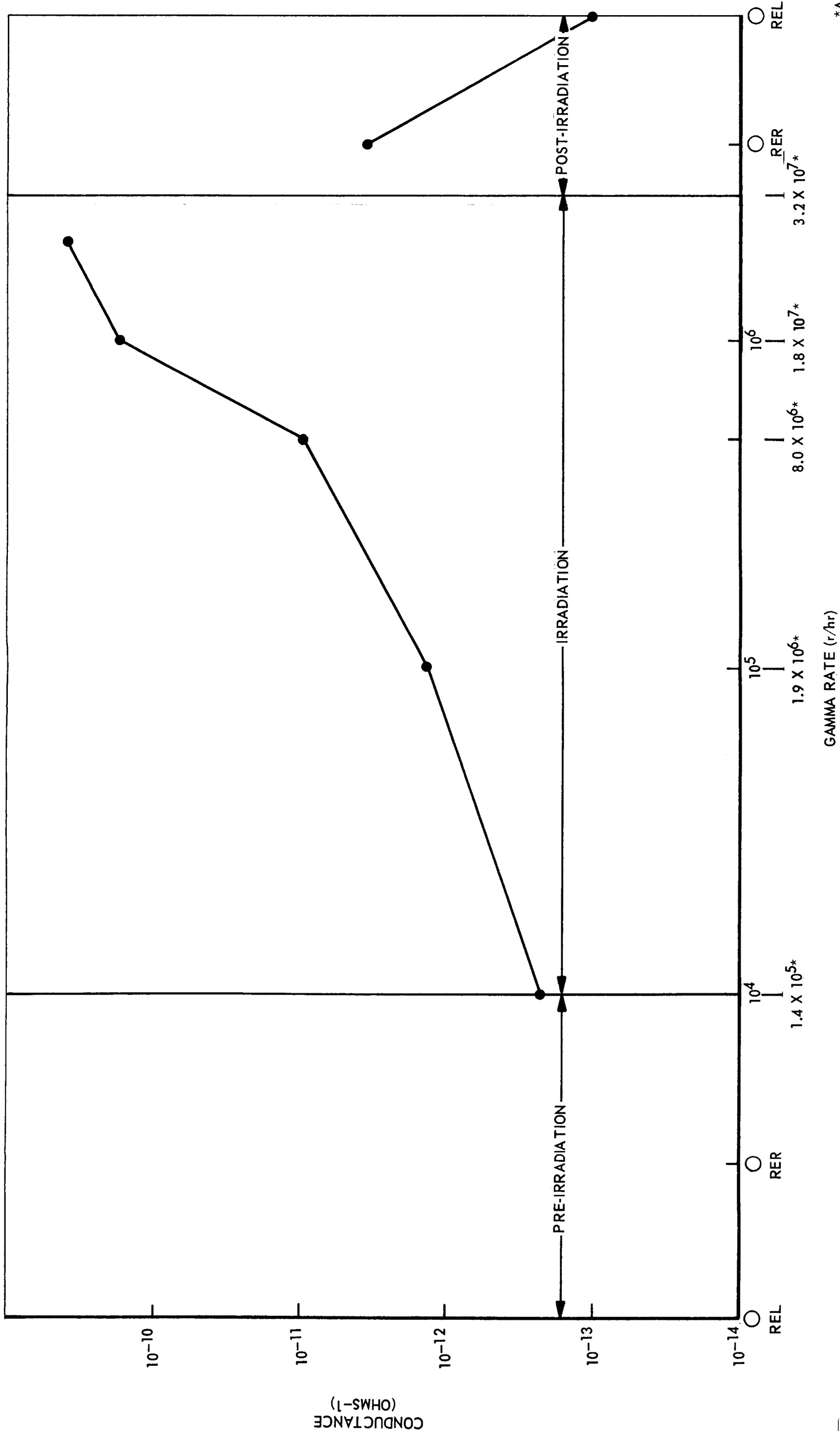
Figure 4-10 represents the photovoltaic current as calculated using equation (2) of paragraph 4.2.1.

RG-58C/U. The induced conductivity of RG-58C/U was found to increase by a factor of 10 when the temperature was raised from 12°C to 70°C; this is shown in Figure 4-11. A saturation effect was noted at dose rates greater than 5×10^5 r/hr at 70°C, which did not occur in the earlier test at 12°C. This phenomenon is explained by the conduction-band model, in which the energy gap between electron energy levels becomes successively filled by the increasing temperature; whereas, the electrons being applied by the increasing radiation do not have enough energy to pass into the next energy band,



NSP 6888

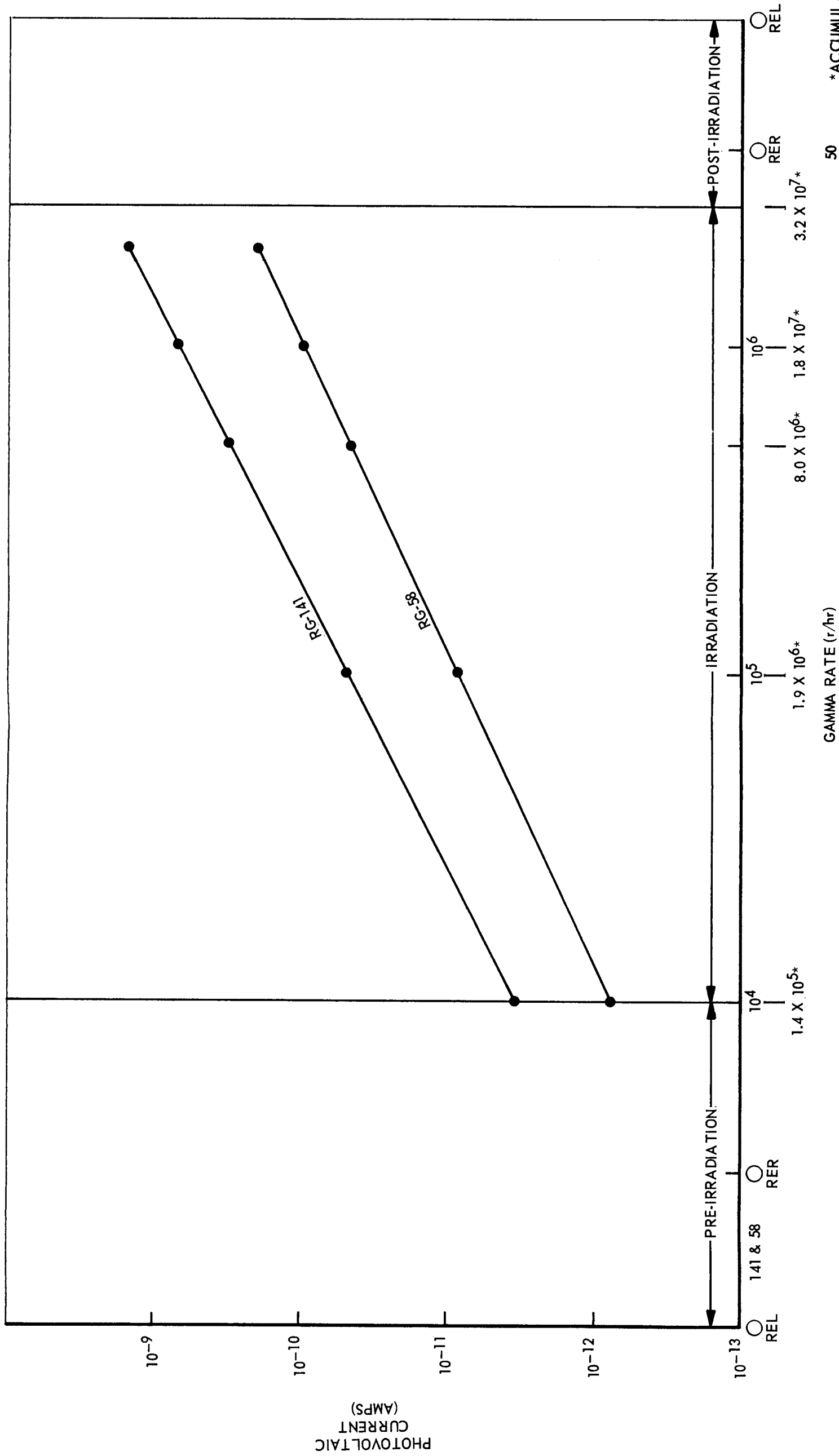
Figure 4-8 Leakage Conductance per Lineal Foot vs Gamma Rate -- RG-58C/U



NSP 6889

*ACCUMULATED DOSE

Figure 4-9 Leakage Conductance per Lineal Foot
vs Gamma Rate -- RG-141



NSP 6890

Figure 4-10 Photovoltaic Current per Lineal Foot vs Gamma Rate -- Coaxial Cable

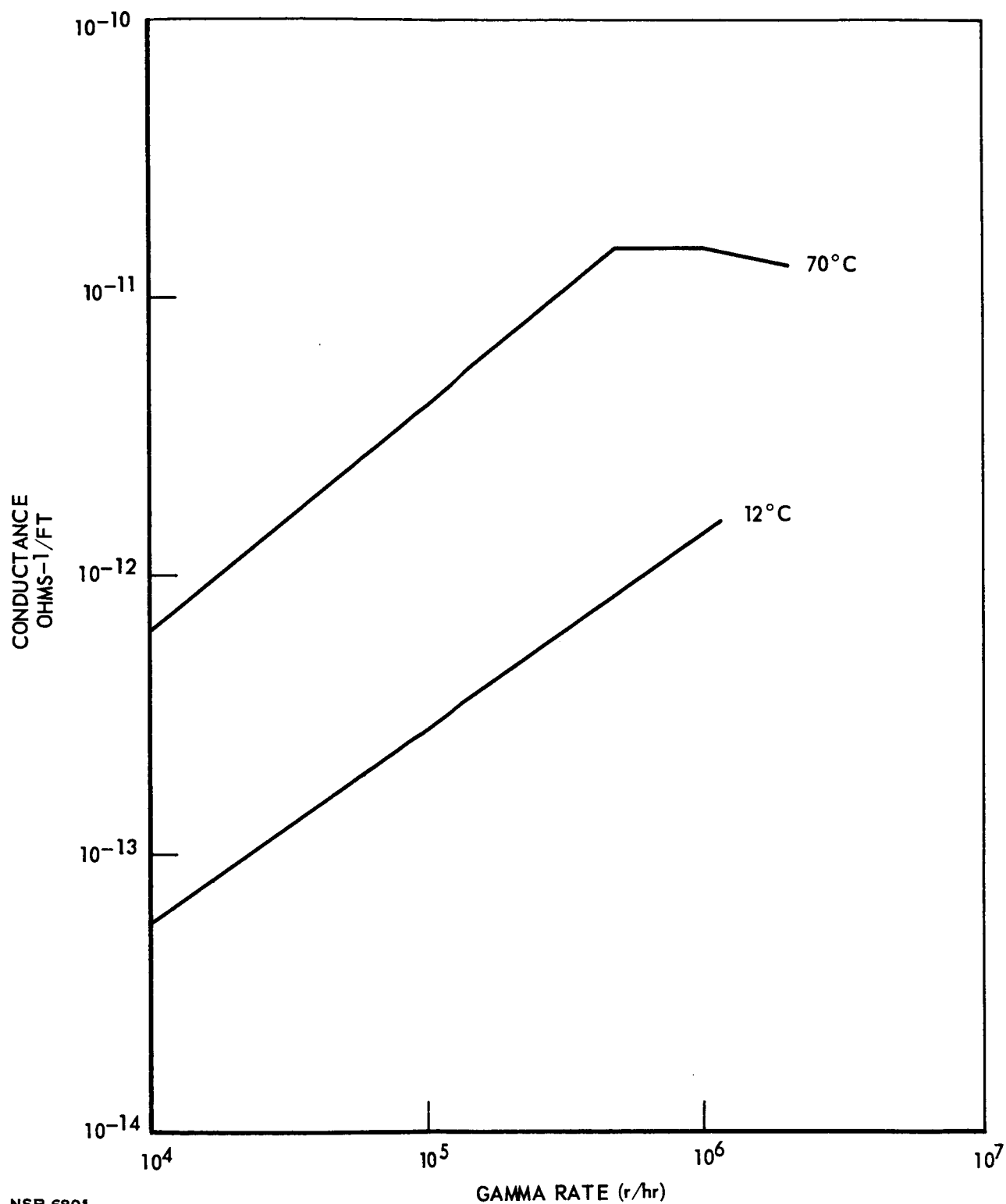


Figure 4-11 Conductance of RG-58C/U Cable at 12 and 70°C

and therefore cannot increase the conductance of the system. Temperature alone appears to have no permanent effect on the cable. There appears to be a slight total-dose effect on the cable, but the data do not permit a quantitative evaluation.

The current measured at zero voltage follows the basic equation of $i = K_1 \gamma \Delta$. The current increased approximately 2 decades from 10^{-12} to 10^{-10} amperes while going from a dose rate of 10^4 to 2×10^6 . The cable was monitored for r-f noise at 400 mc, and no noise was detected above the 10-db noise level of the measuring equipment.

RG-141/U. The conductance of RG-141/U (Teflon FEP) increased rapidly with increasing exposure, and then began to taper off at the higher dose rates. Since Teflon is normally damaged at integrated doses of 5×10^6 , it is believed that part of the effect is due to the additional phenomenon of materials degradation, and the electrical model alone, is insufficient to interpret the experimental results. The pre- and post-irradiation measurements indicate that permanent change has occurred in the Teflon. There was no change in the conductance of the control specimens.

The photovoltaic current at zero voltage followed the empirical relation $i = K_1 \gamma \Delta$. Once again the current measured is not a measure of the total charge produced; measurements should be made at different applied voltages in any future tests.

The cable was monitored for r-f noise the same as in RG-58C/U; no noise was detected.

4.3.2 Four-Conductor Cables--MD-324 and CDS-47831 (PVC)

The reduced data for the leakage conductance are calculated from the model presented in Section 4.2.1. The calculated data are plotted in Figures 4-12 and 4-13.

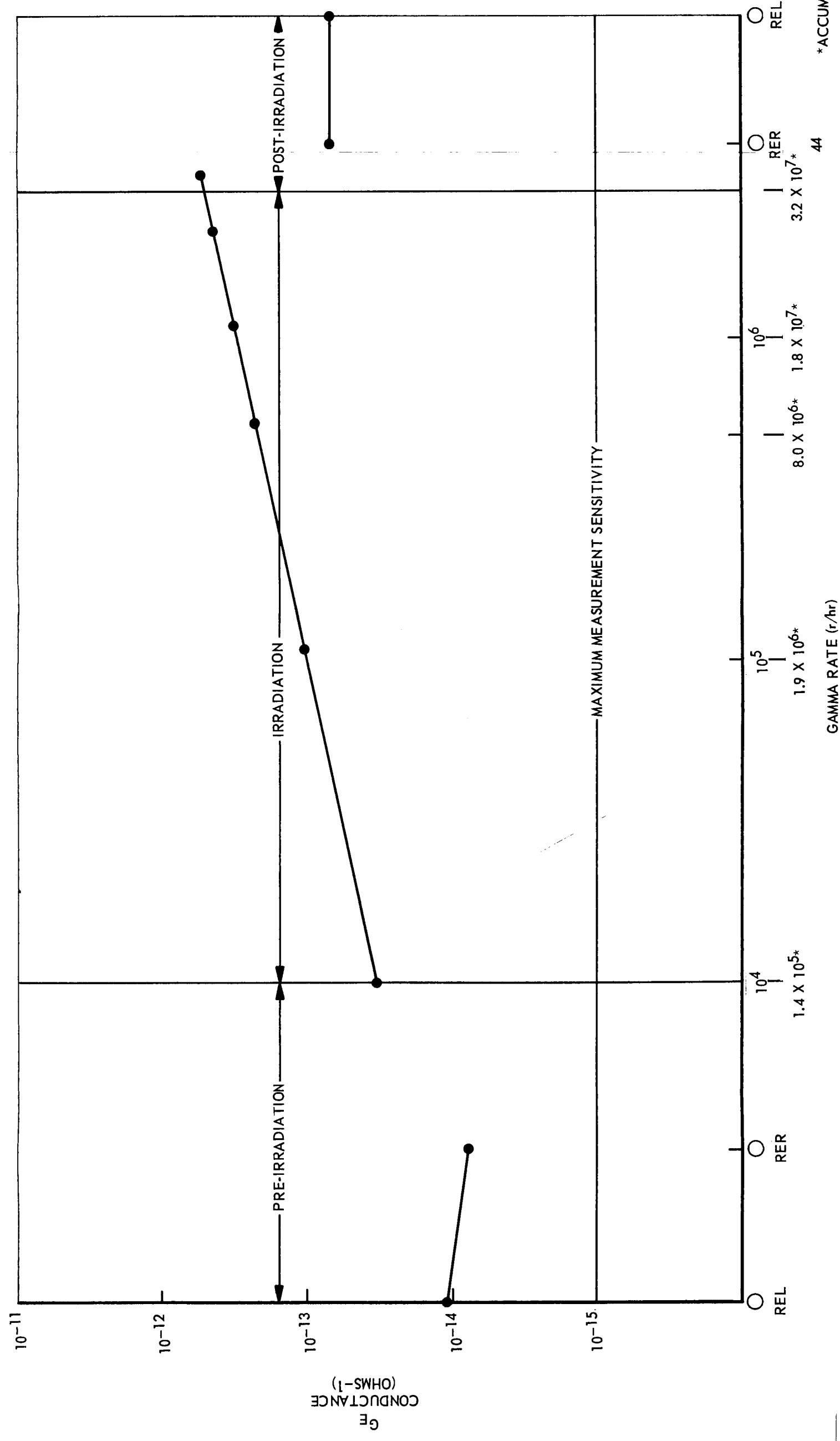
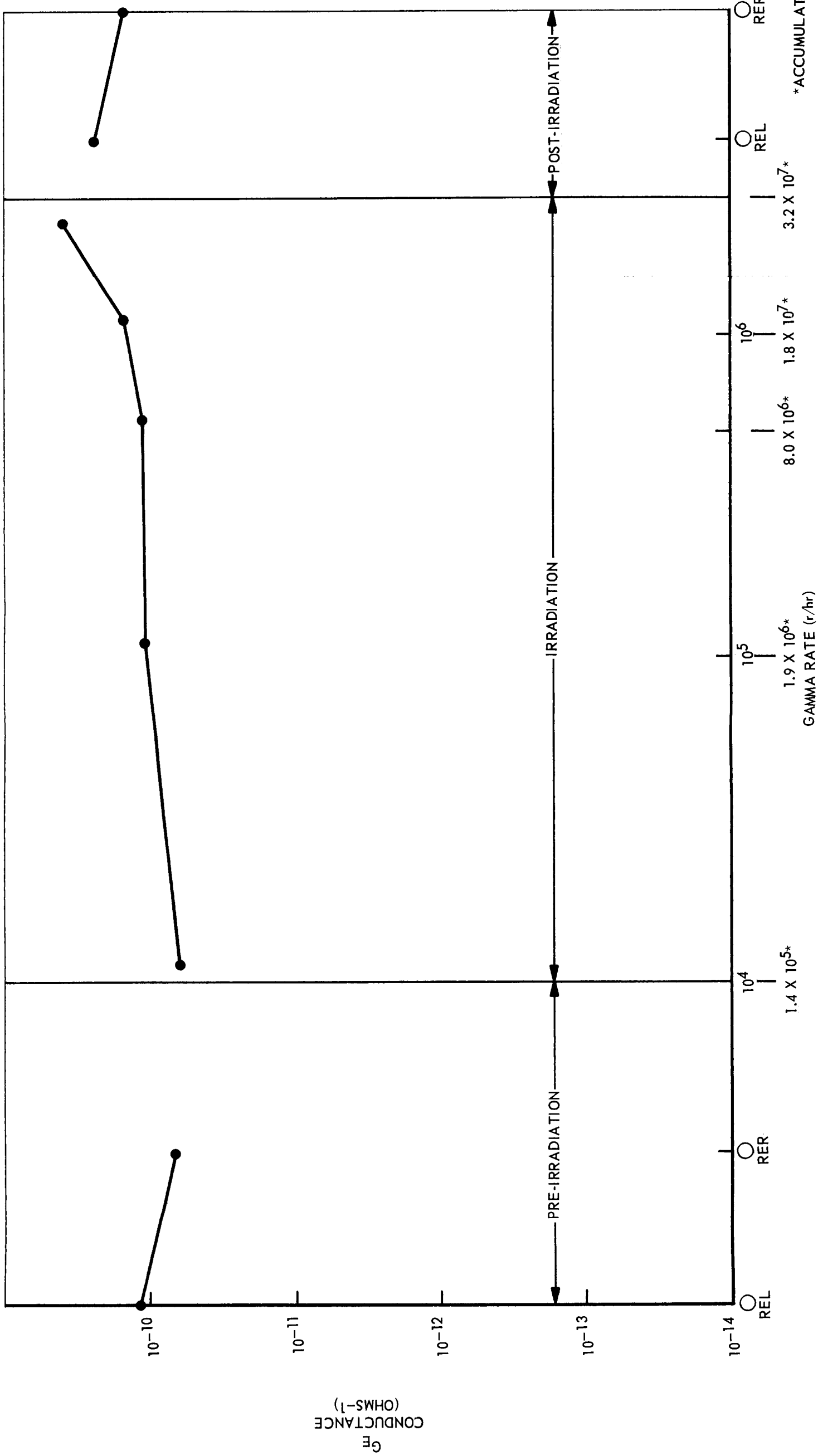


Figure 4-12 Leakage Conductance between Shield and Conductor per Lineal Foot of Cable Type MD 324 vs Gamma Rate



NSP 6893

Figure 4-13 Leakage Conductance between Shield and Conductor per Lineal Foot of Cable Type CDS 47831 (PVC) vs Gamma Rate

The pre- and post-irradiation data, and the control data are also plotted in Figures 4-12 and 4-13.

The photovoltaic current for CDS-47831 (PVC) at zero voltage is plotted in Figure 4-14.

MD-324. The MD-324 four-conductor cable showed an increase of approximately ten in conductance with the radiation rate going from 10^4 to 2×10^6 . The pre- and post-irradiation showed a slight permanent change of no great significance. Temperature alone showed no effect. The photovoltaic current at zero voltage could not be calculated because of the erratic distribution of the experimental data. Hence, no curve is shown.

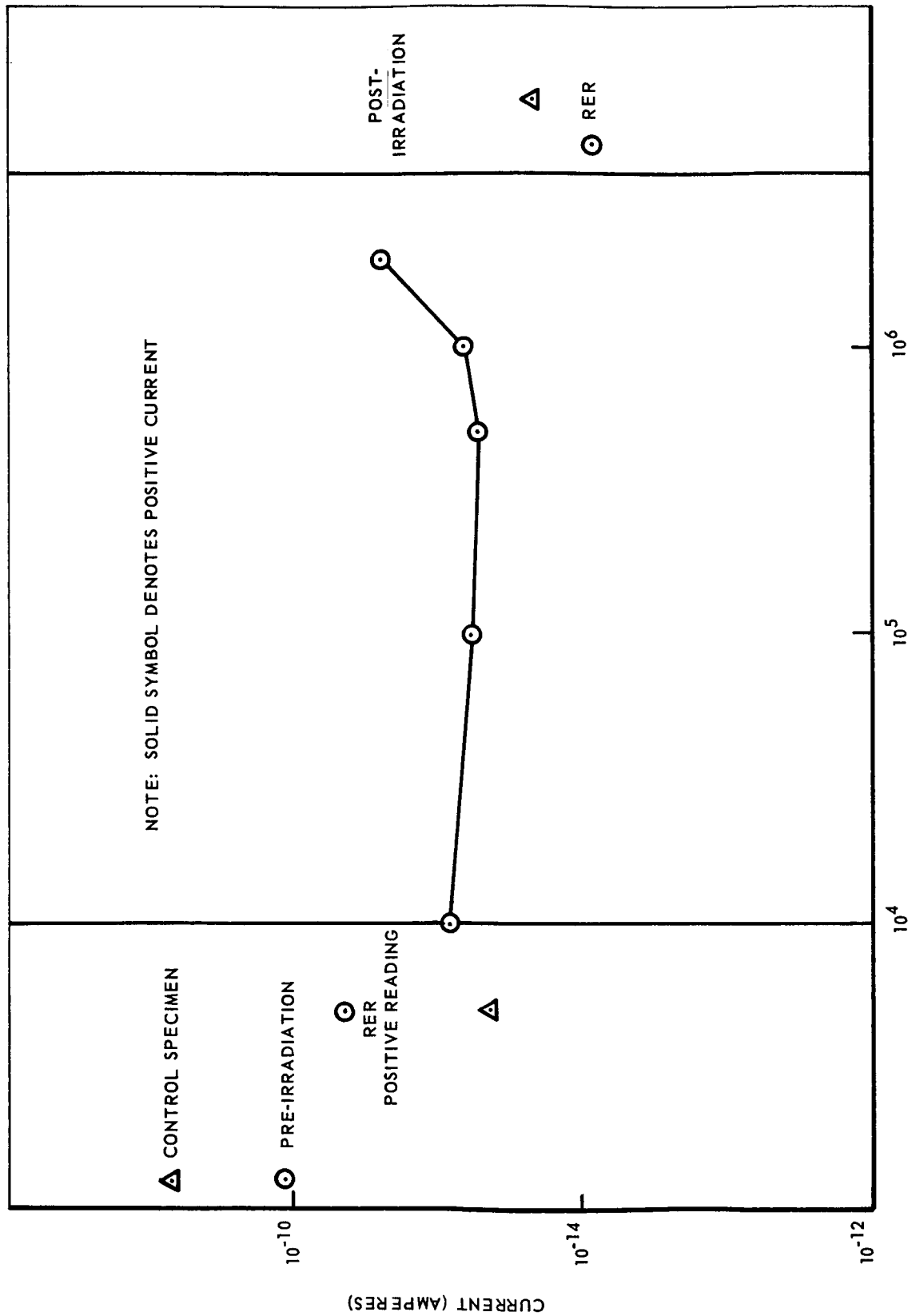
CDS-47831 (PVC). The conductance of this cable was essentially unaffected by the radiation rate. The cable also showed no effect of time at test temperature or total dosage. The normal leakage conductance is 1000 times higher than that of polyethylene or Teflon cable.

The photovoltaic current does not appear to be a function of radiation dose rate.

Type PSC-C-39001-4-24ST (Silica-Glass). Figure 4-15 presents the conductance as defined by Equation (1) of Section 4.2.1. The data points for Test Samples #1 and #2 have been presented separately because the samples were noticeably different in their physical dimensions; averaging the data was not deemed justified. Due to a short, no conductance data were obtained on Test Sample #3.

The pre- and post-irradiation data do not indicate any total dose effect on the cable. The temperature control samples did not show any change of conductance during the period of the experiment.

The conductance of the PSC cable increased from less than $10^{-15} \text{ ohm}^{-1}$ to not more than $10^{-14} \text{ ohm}^{-1}$ per lineal foot of cable when the temperature



NSP 6894

GAMMA DOSE RATE, r

Figure 4-14 Photovoltaic Current between Shield and Conductor per Lineal Foot of Cable Type CDC 4783I

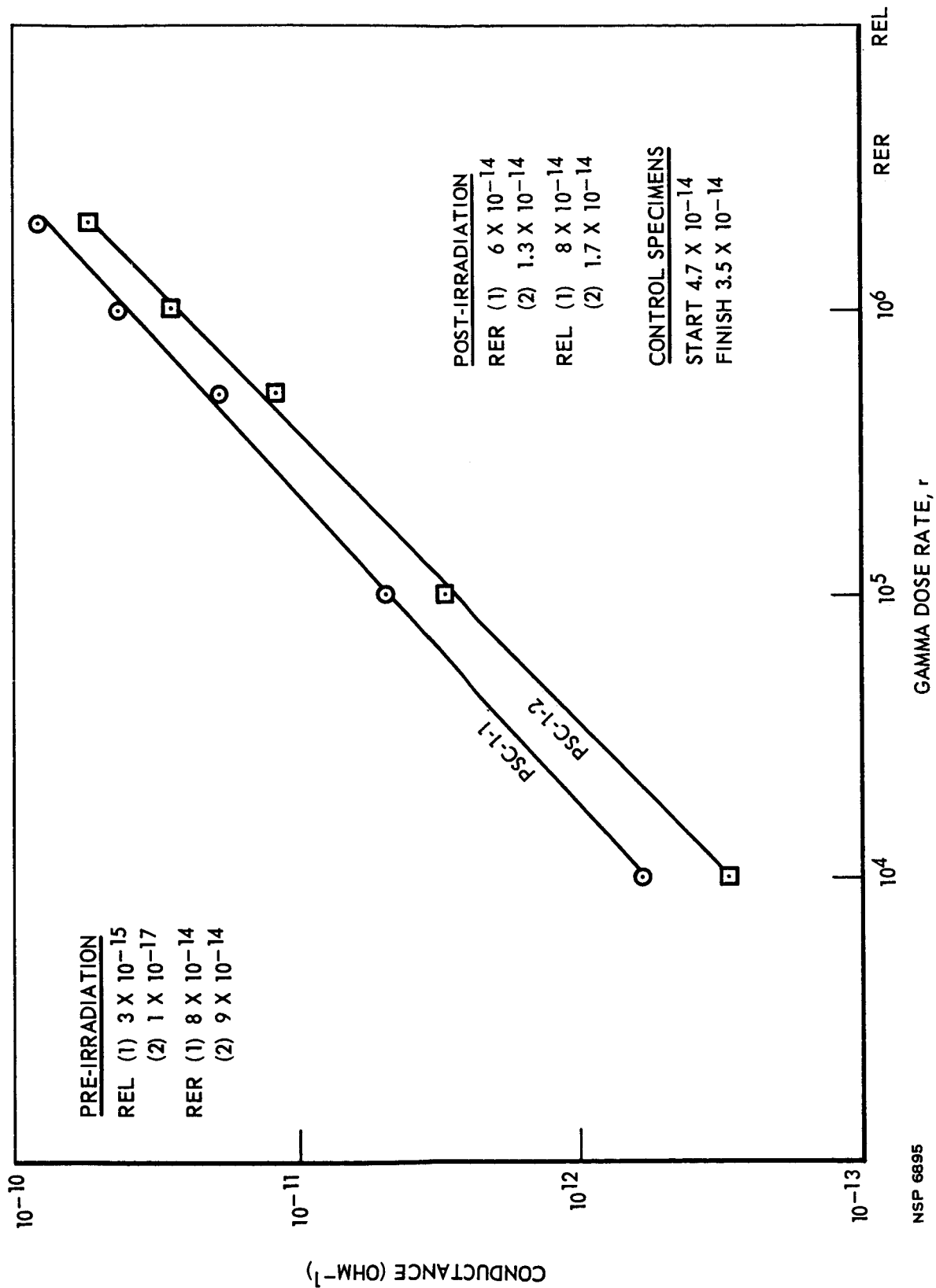


Figure 4-15 Leakage Conductance between Shield and Conductor per Lineal Foot of Cable Type PSC-C-39001-4-24ST

was raised from 20 to 70°C. The empirical relationship $G = K_2 \gamma^\delta$ seems to hold for this cable. However, since the cables were of different size, it appears that, in addition to construction material, a geometric effect affects the constants. The conductance rose two orders of magnitude under the dose rates examined.

The photovoltaic current data were erratic, so no calculations were attempted. The pre- and post-irradiation data as well as the temperature control data showed that there were no significant temperature or total dose effects.

4.3.3 Twisted-Pair Cable

4.3.3.1 Type RT 24(19)ST 2RO/9-0 (Irradiated Polyethylene). Figure 4-16 shows the average leakage conductance between the shield and the conductors per foot of cable for the twisted-pair-type cable RT 24(19)ST 2RO/9-0. The method of obtaining these conductances has been explained.

Figure 4-17 shows the average resultant current per foot of cable. The pre- and post-irradiation conductances and currents do not indicate any total dose effect on the cable. The temperature control specimen did not indicate any ageing effect due to temperature.

The conductance of this cable was unaffected by the radiation rate until 5×10^5 r/hr was reached. The total change from the initial conductance of 2×10^{-13} ohm⁻¹ was a factor of 5 to 9×10^{-13} ohm⁻¹ at a dose rate of 2×10^6 r/hr. The pre- and post-irradiation measurements and temperature control experiment showed that there was no permanent change of the cable caused by the temperature or total dosage. The photovoltaic current rose from 2.5×10^{-12} to 8×10^{-11} amperes going from 10^4 to 2×10^6 r/hr.

4.3.4 Connector Type PT00P-14-5 S and PT06P-14-5 P—Neoprene.

Figure 4-18 shows the conductance per connector values for the connector (PT00P-14-5 S, the socket, and the PT06P-14-5 P, plug). The method of computing the data points is given in Section 4.2.1.

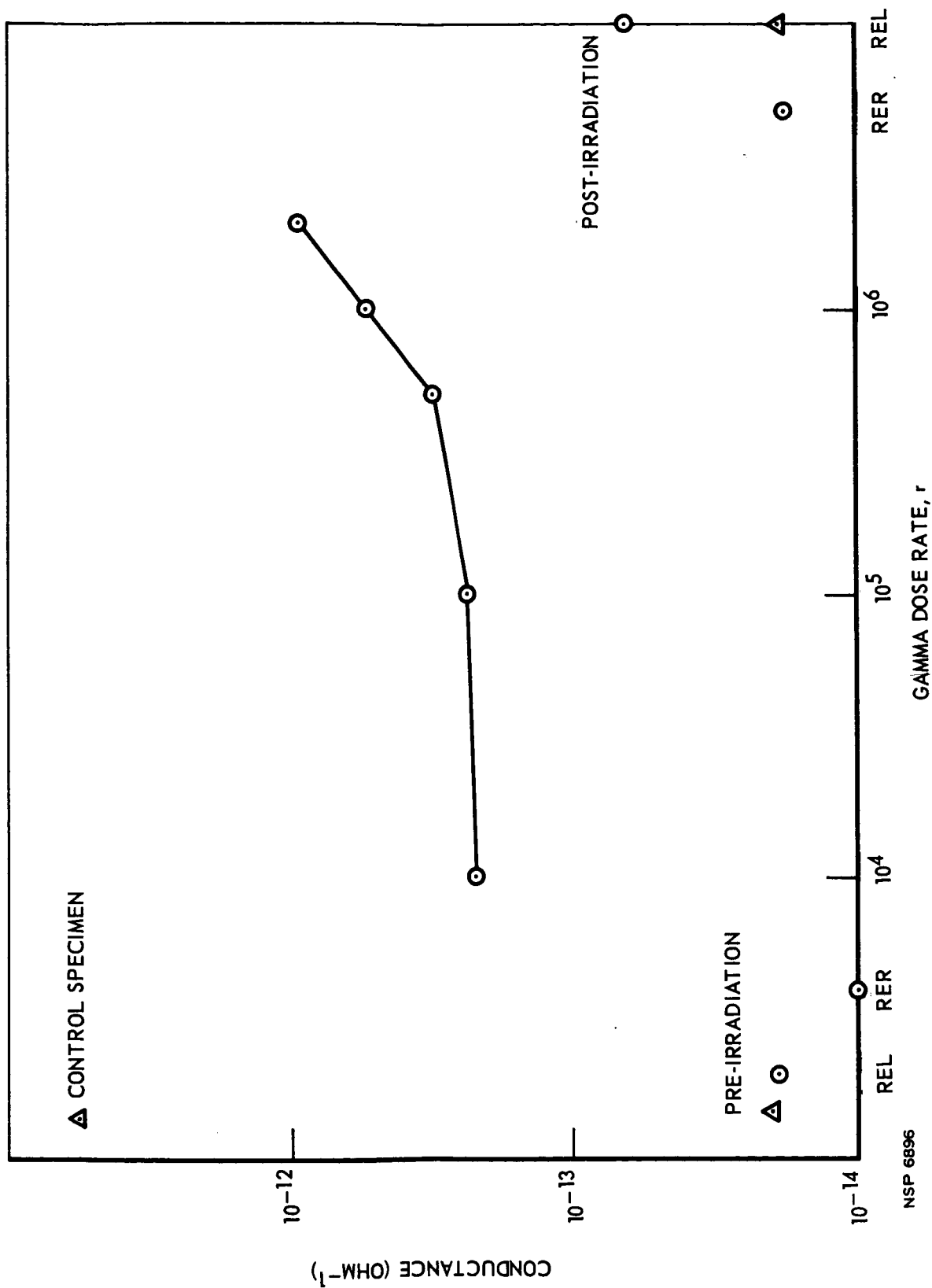


Figure 4-16 Leakage Conductance between Shield and Conductor per Lineal Foot of Cable Type RT 24(19)ST+2R0/9-0

NSP 6896

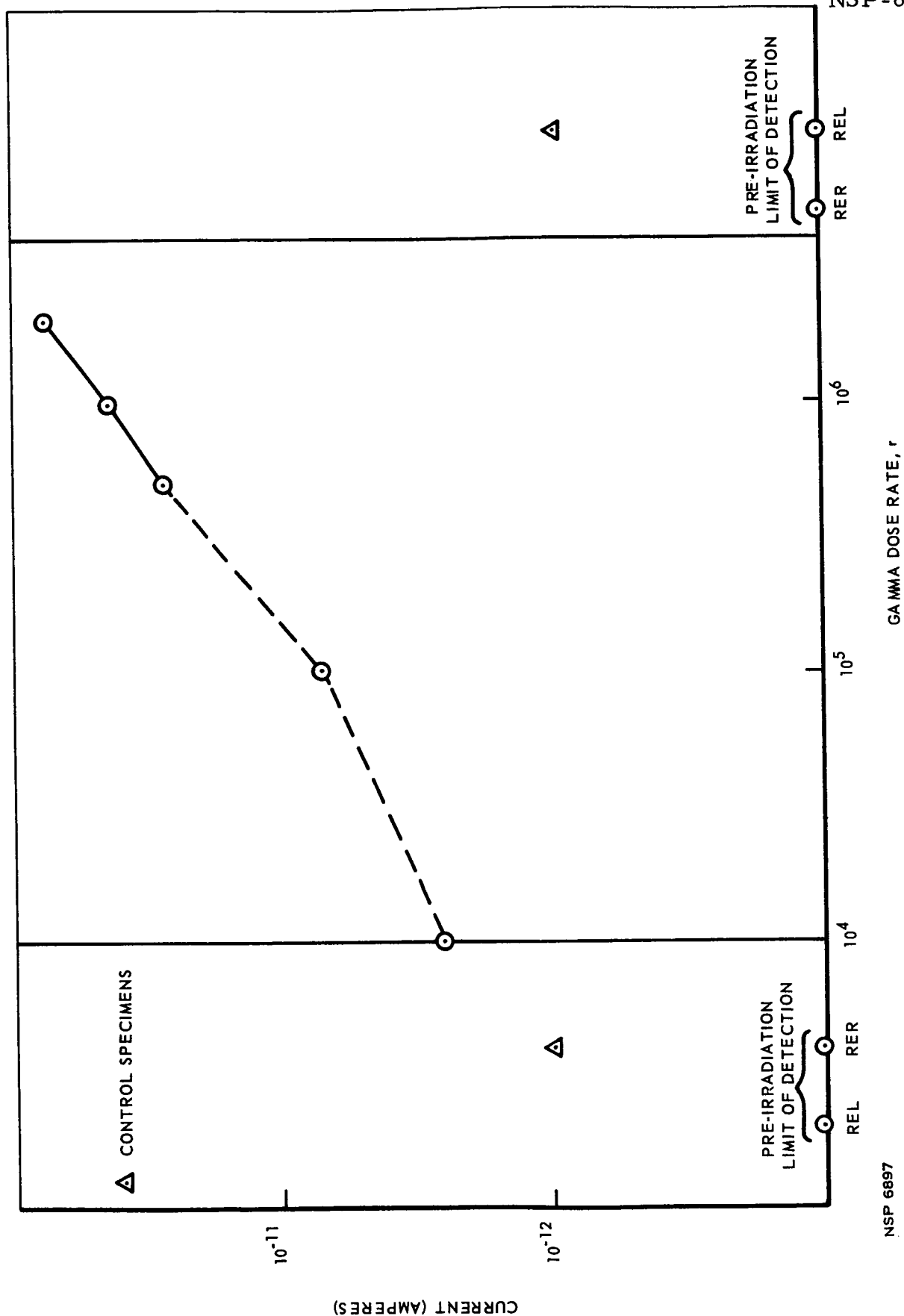
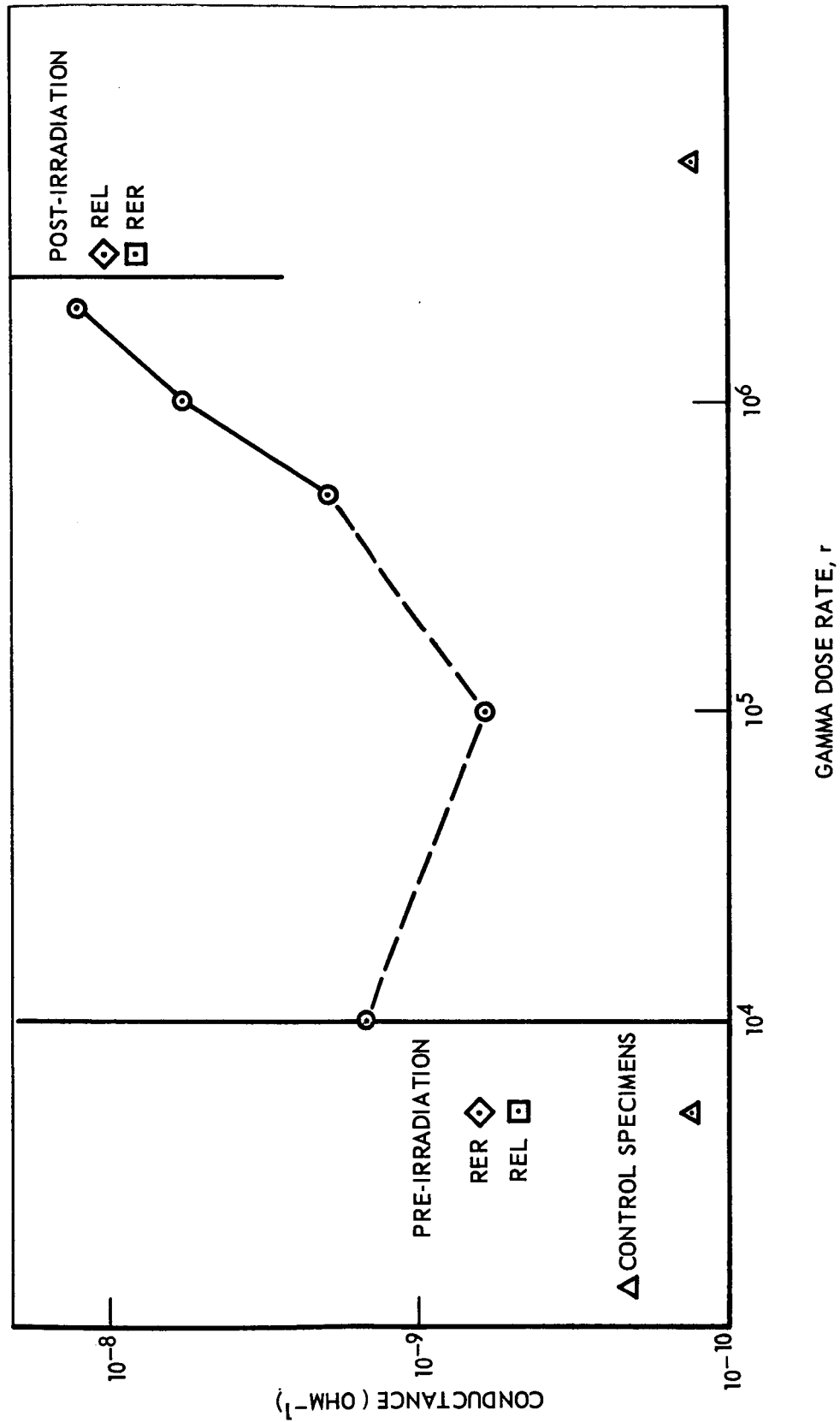


Figure 4-17 Photovoltaic Current between Shield and Conductor per Lineal Foot of Cable Type RT(19)ST-2R0/9-0

NSP 6897



NSP 6898

Figure 4-18 Leakage Conductance between Shield and Conductor Type PT 00P-14-5S and PT 06P-14-5P

Pre- and post-irradiation points are also plotted (marked REL and RER).

Figure 4-19 shows the average photovoltaic current between the exterior case (shield) and conductor (pin) of the connector.

The effect of the 3M #XR 5038 potting compound on the leakage conductance and current are negligible under non-irradiation (dark) conditions.

The temperature control specimens showed no change due to temperature over the period of testings.

The conductance of this connector is complicated by the fact that there appears to be a total dose effect as well as a rate effect. Further, the temperature alone raises the conductance from $6 \times 10^{-15} \text{ ohm}^{-1}$ at ambient temperature to $6 \times 10^{-10} \text{ ohm}^{-1}$ at 70°C . The pre- and post-irradiation data show that a permanent change has occurred in the connector. When the effect started cannot be determined, since it is not possible to separate the dose-rate effect from the total-dose effect with the available data. The control experiment showed that there was no ageing effect during the temperature alone. The photovoltaic current rose from 4×10^{-10} amperes at 10^4 r/hr to 5×10^{-9} amperes at $2 \times 10^6 \text{ r/hr}$. This current was still present after the reactor was shut off showing that temperature and the change of properties of the material are causing current generation.

The relationships of induced currents and conductances to dose rate and material are generally accepted as:

$$i = K_1 \dot{\gamma}^\Delta$$

$$G = K_2 \dot{\gamma}^\delta$$

where $\dot{\gamma}$ is dose rate, K_1 , K_2 , Δ , and δ are empirical constants for the material in question. However, these equations were derived for slab material and experimental data taken under very carefully controlled environmental conditions. The multiconductor cable data obtained in the

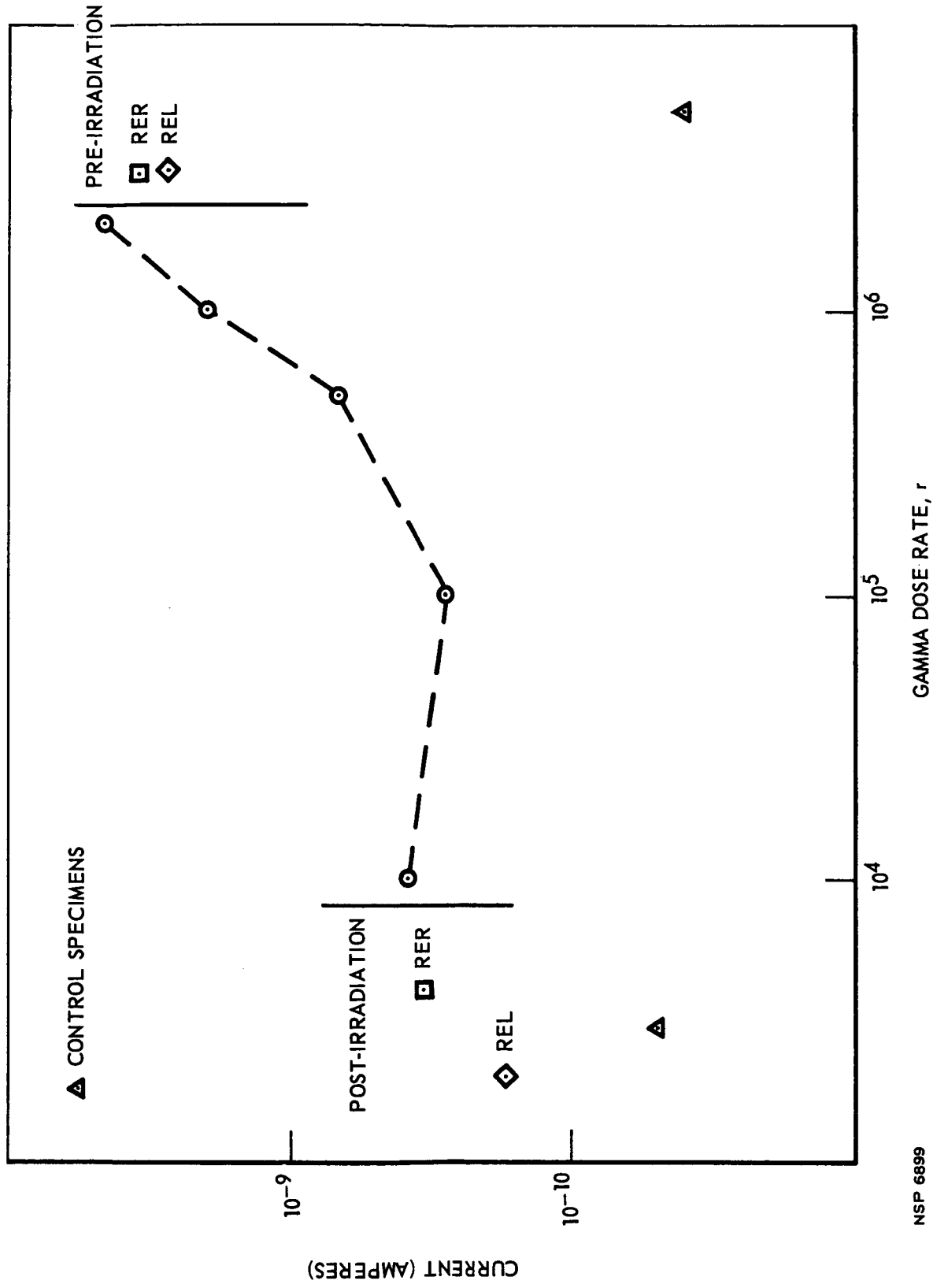


Figure 4-19 Photovoltaic Current between Shield and Conductors per Connector Types PT 06P-14-5P

NSP 6899

present experiments is for more complicated geometric configurations and therefore the above equations may not fit this case. Further, since the current, i , is measured without a bias being applied to the cable, there is no electric field within the cable to give a drift direction to the induced charges. Therefore, not all of the induced charges are swept out and measured as a current, i ; this leads to low measured values of i . Even if the data obtained can be fitted to the above equations, the validity of the approach is questionable. Hence, no attempt has been made to obtain the empirical coefficients for multiconductor cables.

The measurement of currents in the cables before being irradiated requires elucidation at zero potential. The driving force under these conditions can only be supplied by temperature or contact potentials. Since the cables and their associated networks are so long and the temperature varies throughout the system, it is not possible to predict the initial sign of the current generated. Since the initial currents can carry either sign, these assume importance only when the irradiation-induced current is the same order of magnitude.

An example of this above phenomena is already seen in the photovoltaic current of both the RG-58 and RG-141 as plotted in Figure 4-10. The measurement's reversed polarity is going from the REL to RER. Further, not all the cables of the same type have the same polarity in the REL. The initial currents have been measured from 10^{-15} to 10^{-11} amperes while the currents during radiation have varied from 10^{-13} to 10^{-9} . This shows that the thermal and contact potentials can have an important effect on the final results. The effect of temperature is tabulated in Table 4-3. It can be seen from this table that there is practically an order of magnitude change in going from ambient to test conditions.

In all of the cables and connectors examined, there were no permanent temperature effects shown in the elapsed time of the experiments.

Table 4-3
EFFECT OF TEMPERATURE ON CABLE CURRENT (AMPERES)

Location	REL			70°C		RER	
	Ambient					70°C	
Voltage	0	-500	0	-500	0	-500	-500
Cable Designation							
Connectors							
MD-1	-	-1.8(-8)	8.6(-10)	-1.2(-6)	1.7(-9)	-1.6(-6)	
MD-2	-	-1.8(-8)	8.1(-10)	-1.2(-6)	1.8(-9)	-1.5(-6)	
Multiconductor							
MD-3	-	-2.5(-10)	-	-3.6(-11)	-	-4.6(-10)	
PSC 1	-	-2.6(-10)	-	-8.2(-10)	2.9(-11)	-1.6(-9)	
PSC 2	-	-2.6(-10)	-	-3.6(-9)	-	-1.2(-9)	
PSC 3	-	-2.9(-10)	-	-2.2(-9)	-	Short	
PSC 4	-	-2.2(-10)	-	-6.0(-10)	-	-1.4(-9)	
Two-Conductor							
RT-1	-	-3.5(-11)	-	-1.8(-10)	-	-5.5(-10)	
RT-2	-	-3.4(-11)	-	-1.7(-10)	-	-6.2(-10)	
RT-3	-	-4.0(-11)	-1.4(-11)	-2.3(-10)	-1.2(-11)	-9.2(-10)	
RT-4	-	-4.3(-11)	-1.3(-11)	-3.5(-11)	-1.5(-11)	-1.2(-10)	

4.4 FURTHER DISCUSSION OF RESULTS

4.4.1 Factors Influencing Results

In addition to the comments made regarding test results in the previous section, it is appropriate to emphasize that a simple mathematical model has been used, but it is recognized that deviations from that model exist in the real case. In some cases the irregular dependence of the electrical characteristics as a function of the radiation rate is difficult to explain. There is definite evidence of synergistic effects for the RG-58C/U during irradiation at elevated temperature. Resolution of the apparent trends at the high dose rate should be made at still higher dose rates and at other temperature levels.

Section 5
CONCLUSIONS

A number of cables have been examined to determine the change of conductance and photovoltaic currents produced by the rate of the gamma flux, total dose, and temperature of 70°C. It was found that the empirical equation developed for slab geometry of dielectrics was not fully applicable to the multiconductor cables examined. However, the maximum current generated under the environmental conditions examined was 2×10^{-9} amperes which is about three orders of magnitude below most signals that will be generated under vehicle operation in RIFT. It is therefore concluded that any one of these cables will be suitable for general use in RIFT.

The PT connector under the conditions examined warrants a qualified approval, since the data indicated that permanent damage was occurring in the dielectric (Neoprene).

Radio-frequency noise should cause no problems in the RIFT program, since the test indicated that the noise level was below 10 db in the cables examined.

Section 6
REFERENCES

1. J. C. Pigg and C. C. Robinson, "Effect of Reactor Radiation on Electrical Insulation"; Oak Ridge National Laboratory, ORNL 1945 (January 1956)
2. H. W. Wicklein, "Transient Radiation Effects in Coaxial Cables due to Gamma-Neutron Radiation Pulses"; Boeing Airplane Company, D2-90172 (1962)
3. J. A. J. van Lint, "Transient Radiation Effects on Coaxial Cables"; General Atomics Division of General Dynamics, GA-3616 (18 December 1962)
4. S. E. Harrison, "A Study of Gamma-Ray Photoconductivity in Organic Dielectric Materials"; Sandia Corporation, SCDC-2580
5. RIFT Radiation Effects -- Irradiations 1 and 3"; Lockheed Missiles and Space Company, NSP 63-39 (May 1963)
6. "RIFT Radiation Test Program, Cables and Connectors"; Lockheed-Georgia Radiation Effects Facility, NO-308 with Amendment I (23 January 1963)
7. "Neutron Spectral Measurements of the Radiation Effects Reactor Leakage Flux"; Lockheed-Georgia Radiation Effects Facility, NR-100 (August 1960)